Authentication of antibiotics using portable near infrared spectroscopy and multivariate data analysis

Journal:	*Applied Spectroscopy*
Manuscript ID	ASP-20-0191.R1
Manuscript Type:	Submitted Manuscript
Date Submitted by the Author:	n/a
Complete List of Authors:	Assi, Sulaf; Liverpool John Moores University, Pharmacy and Biomolecular Sciences Arafat, Basel; Anglia Ruskin University Faculty of Health Social Care and Education Lawson-Wood, Kathryn; PerkinElmer Inc Robertson, Ian; PerkinElmer Inc
Manuscript Keywords:	counterfeit medicines, antibiotics, near infrared spectroscopy, principal component analysis, soft independent modelling of class analogy
Abstract:	Counterfeit medicines represent a global public health threat warranting the development of accurate, rapid and non-destructive methods for their identification. Portable near-infrared spectroscopy near-infrared spectroscopy offers this advantage. This work sheds light on the potential of combining NIRS with Principal Component Analysis (PCA) and Soft Independent Modelling of Class Analogy (SIMCA) for authenticating branded and generic antibiotics. A total of 23 antibiotics were measured 'non-destructively' using a portable NIR spectrometer. The antiobiotics corresponded to six different active pharmaceutical ingredients being: amoxicillin trihydrate and clavulanic acid; azithromycin dihydrate; ciprofloxacin hydrochloride; doxycycline hydrochloride and ofloxacin. NIR Spectra where exported into Matlab R 2018b where data analysis was applied. The results showed that the NIR spectra of the medicines showed characteristic features corresponds to the main excipient(s). When combined with PCA, NIRS could distinguish between branded and generic medicines and could classify medicines according to their manufacturing sources. The PCA scores showed the distinct clusters corresponding to each group of antibiotics whereas the loadings indicated which spectral features were significant. SIMCA provided more accurate classification over PCA for all antibiotics except ciprofloxacin which products shared many overlapping excipients. In summary, the findings of the study demonstrated the feasibility of portable NIRS as an initial method for screening antibiotics.

Authentication of antibiotics using portable near infrared spectroscopy and multivariate data analysis

Sulaf Assi[1,*], Basel Arafat[2], Kathryn Lawson-Wood[3] and Ian Robertson[3]

1 Pharmacy and Biomolecular Science, Liverpool John Moores University, Byrom Street Campus, L3 3AF, UK; E-Mail: s.assi@ljmu.ac.uk

2 Faculty of Health, Education, Medicine and Social Care, Bishops Hall Lane, Chelmsford, CM1 1SQ, UK; E-Mail: basel.arafat@anglia.ac.uk

3 Perkin Elmer, Chalfont Road, Seer Green, Buckinghamshire, HP9 2FX, UK; E-Mails: Kathryn.lawson-wood@perkinelmer.com; ian.robertson@perkinelmer.com

*Author to whom correspondence should be addressed; Email: s.assi@ljmu.ac.uk; Tel: +44-1519046144

Abstract

Counterfeit medicines represent a global public health threat warranting the development of accurate, rapid and non-destructive methods for their identification. Portable near-infrared spectroscopy near-infrared spectroscopy offers this advantage. This work sheds light on the potential of combining NIRS with Principal Component Analysis (PCA) and Soft Independent Modelling of Class Analogy (SIMCA) for authenticating branded and generic antibiotics. A total of 23 antibiotics were measured 'non-destructively' using a portable NIR spectrometer. The antiobiotics corresponded to six different active pharmaceutical ingredients being: amoxicillin trihydrate and clavulanic acid; azithromycin dihydrate; ciprofloxacin hydrochloride; doxycycline hydrochloride and ofloxacin. NIR Spectra where exported into Matlab R 2018b where data analysis was applied. The results showed that the NIR spectra of the medicines showed characteristic features corresponds to the main excipient(s). When combined with PCA, NIRS could distinguish between branded and generic medicines and could classify medicines according to their manufacturing sources. The PCA scores showed the distinct clusters corresponding to each group of antibiotics whereas the loadings indicated which spectral features were significant. SIMCA provided more accurate classification over PCA for all antibiotics except ciprofloxacin which products shared many overlapping excipients. In summary, the findings of the study demonstrated the feasibility of portable NIRS as an initial method for screening antibiotics.

Keywords

Counterfeit medicines; antibiotics; near-infrared spectroscopy; principal component analysis; soft independent modelling of class analogy

Introduction

Medicine counterfeiting represents a global expanding problem with increased morbidity and mortality worldwide. The impact of counterfeit medicines can result in lethal consequences in its worst. A counterfeit medicine is defined by the World Health Organization (WHO) as "deliberately/fraudulently misrepresent their

identity, composition or source" [1]. A substandard medicine is also known as poor quality medicine that fail to satisfy its manufacturing specifications [1-3].

Medicine counterfeiting can occur to any class of medicines, of any formulation and of any source. Antibiotics represent one of the main classes of medicines sold in both developed and developing countries; thus, have high probability of being substandard or counterfeited [4-8]. Counterfeit and substandard antibiotics may not be limited to the lack of active pharmaceutical ingredients (APIs) but also may have defects in their excipients' constituents or in their physical characteristics .The consequences of using counterfeit antibiotics can range from decreased efficacy [9,10]; treatment failure [11-14]; antimicrobial resistance development [5,15]; and/or lethal consequences [10,15-16].

The literature revealed various methods for antibiotics authentication. These methods range from simple color tests to mass spectrometric methods. Color tests and thin layer chromatography have been used for detecting macrolides [17]; amoxicillin and co-trimoxazole [18]; and fluoroquinolones [19]. Likewise, inexpensive test cards were used for determination of beta-lactam antibiotics [20]. Color tests were also used alongside both the dissolution testing and the Global Pharma Health Fund (GPHF) Minilab for screening of specific classes of antibiotics such as amoxicillin and co-trimoxazole [18] and/or multiple classes [21,22]. More sophisticated techniques used for analysis of counterfeit and substances antibiotics included high performance liquid chromatography [18,23-25], ultra-high performance liquid chromatography [26], liquid chromatography mass spectrometry [27] and capillary electrophoresis [28].

However, all the aforementioned techniques were destructive to the samples analysed and/or required extensive method development. Portable near-infrared spectroscopy (NIRS) offers an advantage over the previous mentioned techniques in being rapid, mobile, and non-destructive. NIRS offers a further advantage over alternative chemical techniques in being able to characterize the physical properties alongside the chemical characteristics of the samples analyzed. Limited studies utilized NIRS for authenticating antibiotics such as ciprofloxacin [29,30]; fluoroquinolones [31]; macrolides [32]. However, the three aforementioned studies

focused on one class of antibiotics and utilized one multivariate data analysis algorithm at a time. Thus, there is still a need to look at a collective method that can authenticate diverse classes of antibiotics synchronously. This work aimed to evaluate NIRS and multivariate classification algorithms for authentication of antibiotics purchased worldwide.

Theory

Spectral pre-treatment

Multiplicative Scatter Correction – First Derivative (MSC-D1) spectral pre-treatment approach was applied in order to correct for the offset and baseline in the spectra that changes depending on several factors including the sample age, thickness and optical properties; temperature; moisture content; and performance of the instrument [33,34]. MSC corrected the offset of the scattered light by construction of a new spectrum that is a linear combination of the original spectrum according to the equation [35,36]:

$$y_{MSC,i} = \frac{(y_i - a)}{b}$$

Where : *yMSC,i* is the corrected spectrum value

yi is the original spectrum value

a is the intercept of the line

b is the slope of the line

First derivative was corrected both the offset and baseline of the NIR spectra using Savitzky-Golay method where a second order polynomial was fitted to the data by least square using 13 data points [35].

Correlation in Wavenumber Space (CWS)

CWS method matched the correlation coefficient (r) value of the test spectrum (A) and a reference spectrum (B). It was calculated as the momentum product (r_p) between both spectra according to the equation [35,37]:

$$r_p = \frac{\sum(A_i - \bar{A})(B_i - \bar{B})}{\sqrt{\sum(A \quad ^{-} \quad \sum(B_i - \bar{\ })^2}}$$

An r value of -1 meant that the spectra were completely dissimilar whereas an r value of +1 meant that the spectra were identical. In this work, an r value of 0.95 was taken as a match among products because it was difficult to get +1 among identical samples due to noise in the spectra [35,37]. For evaluation of CWS method, type I and type II errors were explored [30]. Type I errors (known as false positives) were encountered when an authentic antibiotic was misidentified by the algorithm (i.e. gave r values < 0.95). On the other hand, type II errors (known as false negatives) were encountered when a counterfeit sample were identified as authentic (i.e. gave r values > 0.95).

Principal Component Analysis (PCA)

PCA classified spectral data by reducing its dimensionality into two subspaces being scores and loadings. The scores showed the distribution of the antibiotics in multidimensional space and the loadings showed significant absorbance values corresponding to the significant constituents (influencers) within the models. PCA was applied to the MSC-D1 NIR spectra of the products in order to visualize patterns on classification among the products. As with CWS method, PCA was evaluated for type I and type II errors [30]. In this case, type I error was encountered when an authentic antibiotic was not clustered with authentic antibiotics. Moreover, a type II error was encountered when a counterfeit antibiotic was clustered with the authentic ones.

Soft Independent Modelling of Class Analogy (SIMCA)

SIMCA is a chemometric approach, based on PCA, which models the variation within the collection of reference spectra for a given material, as well as the difference between spectra of different materials [38]. This allows SIMCA to be sensitive to small spectral differences, even batch-to-batch or sampling variations. New samples can then be classified to one (or none) of the established class models, based on their similarity to the respective model. This is achieved by investigating the size of its residual, as well as its location on the scores map.

Materials and Methods

Materials

A total of 23 antibiotic products containing six different APIs were used in this study (Table 1). The APIs of the antibiotics included: amoxicillin trihydrate and clavulanic acid; azithromycin dihydrate; ciprofloxacin hydrochloride; doxycycline hydrochloride and ofloxacin. The antibiotic products were obtained from 11 different countries: Austria; France; Germany; Ghana; India; Italy; Jordan; Lebanon; Spain; UAE and the UK. The products were either tablets or capsules and included both branded and generic medicines. Regards the excipients, 19 products had between seven and 10 excipients each (Table 2). The excipients of the remaining four products were not reported. In total, 29 excipients were present in at least one or more products (Appendix A). The recurrent excipients were: hypromellose, magnesium stearate, maize starch and titanium dioxide.

Near infrared spectroscopic analysis

NIR spectra of antibiotic products and their individual constituents were collected using the PerkinElmer Spectrum Two N™ FT-NIR instrument equipped with NIR reflectance module (NIRM). Tablet formulations were measured as received from both sides. The contents of each capsule formulation were emptied into glass vials and were measured through the vials. Likewise, excipients were powders and were

measured via glass vials. Two spectra were collected per each tablet and three spectra per each vial over the wavenumber range of 10,000 – 4000 cm^{-1} with spectral resolution of 8 cm^{-1}. Each spectrum was the sum of 32 scans.

Data analysis

Spectra were exported into Matlab R2018b where data pre-treatment was applied. Pre-treatment of NIR spectra was made using MSC-D1. Multivariate data analysis was conducted using CWS; PCA; and SIMCA methods. CWS was applied to the MSC-D1 NIR spectra in Matlab R2018b where the r values of products were compared and an r value of 0.95 was considered a threshold. PCA was applied in Matlab R2018b where clustering among antibiotics was evaluated. SIMCA analysis was carried out using PerkinElmer AssureID™ materials verification software to create five PCA models of the antibiotic products. A global PCA of all materials was also created to provide an overview of the complete model and understand relationships between material types. The threshold taken for inter-material distances was 1.5 where a distance below 1.5 was considered a similarity.

Results and Discussion

Diversity of the sample set relating to the APIs and excipients

In order to evaluate the identification potential of the method, 23 antibiotic products relating to five APIs were chosen. The products were of both branded and generic types, of tablet and/or capsule formulations and were obtained from different sources across the wholesale supply chain including community pharmacies, hospital pharmacies, humanitarian aid supply, online pharmacies, street market and wholesalers (Table 1). The APIs of the evaluated products were: amoxicillin trihydrate and clavulanic acid (AMC); azithromycin dehydrate (AZ); ciprofloxacin hydrochloride (CIP); doxycycline hydrochloride (DOX) and ofloxacin (OFL). The numbers of products per antibiotic varied between two and 12 products for each API depending on availability and were: Two for each of DOX and OFL, three for AMC, four for AZ, and 12 for CIP. In some cases, the aforementioned products had

overlapping excipients (Table 2). Excipients were always reported for branded but not generic products. Where reported, the minimum number of excipients per product was six and the maximum was 10. However, in most cases the main excipients were consistent among products of the same API. For instance, AMC products (AMC1, AMC2 and AMC3) were from three different manufacturers in Lebanon, Spain and the UK and had overlapping excipients being: hypromellose, microcrystalline cellulose (MCC), magnesium stearate (MgS), and titanium dioxide. Likewise, OFL products (OFL1 and OFL2) were from two different manufacturers and had six common excipients being: croscarmellose sodium, hypromellose, lactose, maize starch, MCC, and titanium dioxide. CIP branded products (CIP1-CIP5) were all from the same manufacturer and had the same list of excipients. Three generic CIP products (CIP7, CIP8, and CIP9) had common excipients as branded CIP products being: crospovidone, colloidal anhydrous silica, hypromellose, macrogol 4000, maize starch, MgS, MCC, and titanium dioxide. On the other hand, AZ products (AZ1, AZ2, AZ3, and AZ4) were manufactured by two manufacturers and showed different excipients between both manufacturers. Moreover, CIP11 and CIP12 had different list of excipients to the other CIP products. The excipients were not reported for CIP6, CIP10, DOX1, and DOX2 that were manufactured by generic manufacturers.

Spectral evaluation

The spectra of the antibiotic products showed characteristics for their main excipients that were key in identifying the products using NIRS (Appendix B). Hence, NIRS offered the advantage of giving more information on the samples' constituents including the API and excipients. Thus, it could serve as a fingerprinting in spectral identification [39]. This was confirmed when the branded medicine of each antibiotic was compared against its main excipient (Figure 1). However, the degree of match depended on the amount of API or excipients in the product. OFL1 showed spectral similarity for MCC and maize starch with correlation coefficient (r) values of 0.73 and 0.69 respectively that confirmed that these excipients were present in adequate amounts. Likewise, DOX1 showed

spectral similarity for MCC and maize starch with r values of 0.71 and 0.75 respectively. However, excipients that were present in low amounts within a tablet did not show peaks in the NIR spectra of the tablets. For instance, talc was present in OFL1 but no characteristic peak for it was seen within its spectra.

Authentication of branded antibiotic products

PCA was successful in showing the chemical variation between different antibiotics. The PCA model showed good classification following MSC-D1 treatment of the NIR spectra of the products. The first three PCs contributed to 89.2% of the variance with 76.4% of the variance explained by PC1 and PC2. Figure 2 shows the 2D and 3D scores plots of AMC1; AZ1; CIP1; DOX1; and OFL1. A distinct cluster was observed for each antibiotic product and that showed the effectiveness of PCA in differentiating between the five authentic products (Figure 2). The highest variance on PC1 was observed for the CIP1 cluster. This was followed by the clusters corresponding to AMC1, DOX1 and OFL1 that were neighboring each other. AMC1 and OFL1 contained around 50% of API and 50% of excipients. Two excipients were common among both products and were MgS and hypromellose. This also could indicate that DOX had similar excipients to AMC and OFL. To interpret the influences of individual constituents on antibiotic products, PC loading plots were visualized. Figure 3 shows the PC1 loading plot of the different antibiotic PCA model that corresponded to 51.2% of the variance. The aforementioned PC1 loading showed contribution over the wavenumber ranges of 9172-8124 cm^{-1}; 7572-6502 cm^{-1}; 6260-5632 cm^{-1}; 5340-4880 cm^{-1}; and 4752-4016 cm^{-1}. The aforementioned five regions showed spectral features corresponding to MgS; ciprofloxacin and MCC; ciprofloxacin and lactose; amoxicillin and ciprofloxacin (Appendix B). This suggested that the five antibiotic products could be principally separated on the basis of differences in their APIs and excipients.

Taking the aforementioned model forward, the next step was to classify the branded and generic medicines for each antibiotic and look into tracking their manufacturing sources (Figures 4 and 5). The discriminative capability of PCA

depended on sample size and sample type [37]. For both AMC and AZ products, two distinct clusters were seen between the branded and generic products (Figure 4 a and b). AMC1, AMC2, and AMC3 showed three distinct clusters that confirmed their three distinct manufacturing sources being the UK, Lebanon, and Spain. The PC1 loading (95.2% of the variance) showed characteristic features for amoxicillin, MCC and talc (Appendix A, Appendix B). Amoxicillin spectral features were seen in the regions of 8910-8378 cm^{-1}; 6178-5636 cm^{-1}; and 5334-5082 cm^{-1}. Talc spectral features were featured at 7318-6992 cm^{-1}; whereas MCC spectral features were seen at 4550-4000 cm^{-1}. Moreover, the PCA scores plot of AZ showed three distinct clusters that corresponded to both their manufacturing sources and formulation type. In this respect, AZ3 and AZ4 products were clustered together where both products were capsules and manufactured by the same manufacturer. Two distinct clusters were seen for AZ1 and AZ2 which were both of tablet formulation but manufactured by two different manufacturers. It is noteworthy to mention here that AZ2 had the same manufacturer as AZ3 and AZ4 but was of tablet instead of capsule formulation. This confirmed the ability of NIR to distinguish physical differences between samples of the same chemical makeup [40]. The PC1 loading plot of AZ products (75.2% of the variance) 7270-7138 cm^{-1} corresponding to talc that was an excipient in AZ1 (of tablet formulation) (Appendix A). Additional spectral features in the PC1 loading plot were seen in the regions of 8804-8350 cm^{-1}; 7074-6800 cm^{-1}; 6584-6290 cm^{-1}; 6064-5646 cm^{-1}; 5334-5004 cm^{-1}; 4984-4668 cm^{-1}; and 4550-4668 cm^{-1}. The aforementioned seven regions corresponded to lactose. DOX products scores plot showed type I error in the cluster of one product (Figure 4c). Hence, DOX1 and DOX2 products were separated in three clusters (instead of two) where DOX1 was separated in two distinct clusters. The PC1 loading of DOX products (90.7% of the variance) showed characteristic features for talc in the region of 7242-7088 cm^{-1}. Other features for this PC1 loading were seen in the region of 6156-5670 cm^{-1}; 5348-4750 cm^{-1}; and 4650-4000 cm^{-1}. The aforementioned three regions corresponded to lactose and MCC. Nonetheless, OFL1 and OFL2 products were clustered into two distinct clusters that corresponded to their manufacturing sources being the UK and France respectively (Figure 4d). However, type I error was encountered in this latter PCA

score plot where both products had outlier(s) within their score plot. The PC1 loading (82.9% of the variance) of OFL products showed characteristic spectral features for talc in the region of 7246-7136 cm^{-1}. Additional peaks were seen in the regions of 6170-5598 cm^{-1}; 5312-5124 cm^{-1}; and 4752-4000 cm^{-1}. The aforementioned three regions corresponded to lactose.

In addition to identifying manufacturing source and discriminating branded from generic medicines; the potential for NIR and PCA for spotting a potential counterfeit product was demonstrated through the PCA scores plot of CIP products (Figure 5). In this sense, the PCA score of a CIP branded product (CIP5) overlapped with one of the generic products. In order to address this overlap, the PC1 loading (67.8% of the variance) of the CIP products had been examined and had shown a major influence of 7260-7150 cm^{-1} that is characteristic for talc [41]. It is noteworthy to mention in this case that talc was not listed in the label claim of any of the branded products. Talc had been found in counterfeit antibiotics as it is cheap and increases the bulk of the medicine [20, 42]. Therefore, CIP5 did not match the manufacturers' specification relating to the identity and could be counterfeit [30].

Development of SIMCA classification models

To further address the type I error encountered with PCA, PCA was taken forward and SIMCA models were constructed. The first SIMCA model showed agreement with PCA Model 1. Hence, distinct classification of the five branded products was observed with no overlapping materials. SIMCA provided a further advantage over PCA in detecting type I and type II errors in classification of different products [43]. In this respect, the distances between the five products were calculated and were found above zero and this showed no type I or type II errors (Table 3). Hence table 3 showed all distances above the threshold that was 1.5. Successively, individual SIMCA models were applied to each antibiotic (Figure 6). For AMC products, the global PCA showed three distinct PCs for AMC1, AMC2, and AMC3 that confirmed their different manufacturing sources. The four AZ products showed three distinct clusters: one corresponding to AZ1, second to AZ2, and the third to AZ3 and AZ4. AZ3 and AZ4 were of the same formulation (both capsules) and had the same

manufacturer but purchased in different countries; therefore, SIMCA was further successful in detecting differences in manufacturing sources and formulation. On the other hand, misclassification was observed among CIP branded and generic products where no clear clustering was observed between both groups of products. Two products were misclassified and seen as two distinct clusters (CIP 6 and CIP 10) and that denoted type I error. Moreover, the aforementioned model could not distinguish the counterfeit CIP batch (CIP 5) that indicated type II error. Likewise, type I error was observed for DOX global PCA where DOX1 was scattered in two distinct clusters. On the other hand, OFL1 and OFL2 products were separated between two individual clusters that corresponded to their different manufacturing sources.

Conclusion

The findings of the study demonstrated the effectiveness of portable NIRS and chemometrics as a tool in authenticating antibiotics. The combination of NIRS with PCA and SIMCA proved to be efficient in discriminating branded from generic medicines and in tracking the manufacturing sources of medicines. Moreover, the algorithms could give initial indication for the presence of a potential counterfeit. However, some limitations were encountered in this study. The first limitation related to sample size and sourcing of the samples that had been a challenge especially that the medicines had been sought from different countries. The second limitation related to the precision of classifying authentic products particularly with large datasets with overlapping excipients such as CIP. Other limitations were associated with the sensitivity of NIRS for characterizing constituents where constituents with low amounts in a medicine will not show spectral features. In summary, portable NIRS could serve as an initial screening method for authentication of antibiotics saving time and money associated with importing the samples to the laboratory. However, for identity confirmation of the API in antibiotics more quantitative techniques are needed.

Acknowledgement

The authors would like to thank Annalene Salter, Adam Naughton, Thomas Coombs and Tiffany Cullern for their contribution to the spectral collection.

Funding

This research did not receive any specific grant from funding agencies in the public, commercial, or not-for-profit sectors.

Conflict of interest

The authors declare that they have no conflict of interest.

References

[1] World Health Organization (WHO). "Definitions of substandard and falsified medical products". Geneva, Switzerland. 2017. https://www.who.int/medicines/regulation/ssffc/definitions/en/. [accessed 21 July 2020].

[2] J. Videau. "Generic drugs: the hidden issues of quality and cost". WHO drug information. 2000. 14(2):77.

[3] World Health Organization (WHO). Quality assurance of pharmaceuticals. Geneva, Switzerland. 1999. https://www.who.int/medicines/areas/quality_safety/quality_assurance/QualityAssuranceePharmVol2.pdf . [accessed 21 July 2020].

[4] H. Frankish. "WHO steps up campaign on counterfeit drugs". The Lancet. 2003. 362(9397):1730.

[5] T. Kelesidis, L. Kelesidis, P. Rafailidis, M. Falagas. "Counterfeit or substandard antimicrobial drugs: a review of the scientific evidence". J Antimicrob. Chemother. 2007. 60:214–236.

[6] World Health Organization (WHO). “Counterfeit drugs: guidelines for the development of measures to combat counterfeit drugs” Geneva: Switzerland. 1999. https://apps.who.int/iris/handle/10665/65892 [accessed21 July 2020].

[7] S. Pincock. “WHO tries to tackle problem of counterfeit medicines in Asia”. BMJ. 2003. 327(7424):1126.

[8] E. Wondemagegnehu. “WHO Report. Counterfeit and substandard drugs in Myanmar and Vietnam”. WHO/EDM/QSM. 1999.

[9] L. Basco, P. Ringwald, A. Manéné, J. Chandenier. “False chloroquine resistance in Africa”. The Lancet. 1997. 350(9072):224.

[10] M. Issack. “Substandard drugs”. The Lancet. 2001. 358(9291):1463.

[11] O. Shakoor, R. Taylor, R. Behrens. “Assessment of the incidence of substandard drugs in developing countries”. Trop Med Int Health. 1997. 2(9):839-845.

[12] D. Menkes. "Hazardous drugs in developing countries: the market may be healthier than the people." BMJ. 1997. 315(7122):1557-1558.

[13] A. Po. “Too much, too little, or none at all: dealing with substandard and fake drugs”. The Lancet. 2001. 357(9272):1904.

[14] B. Stenson, B. Lindgren, L. Syhakhang, G. Tomson. “The quality of drugs in private pharmacies in the Lao People’s Democratic Republic”. Int J Risk Saf Med. 1998.11(4):243-249.

[15] A. Delepierre, A. Gayot, A. Carpentier. “Update on counterfeit antibiotics worldwide; public health risks”. Med Maladies Infect. 2012. 42(6):247-55.

[16] Pharmaceutical Security Institute. “Counterfeit situation”. 2014. http://www.psi-inc.org/counterfeitSituation.cfm. [Accessed 13 June 2019].

[17] C. Hu, W. Zou, W. Hu, X. Ma, M. Yang, S. Zhou, J. Sheng, Y. Li, S. Cheng, J. Xue. “Establishment of a fast chemical identification system for screening of counterfeit drugs of macrolide antibiotics”. J Pharmaceut Biomed. 2006. 40(1):68-74.

[18] I. Fadeyi, M. Lalani, N. Mailk, A. Van Wyk, H. Kaur. “Quality of the antibiotics—amoxicillin and co-trimoxazole from Ghana, Nigeria, and the United Kingdom”. Am J Trop Med Hyg. 2015. 92(6):87-94.

[19] B. Singh, D. Parwate, S. Shukla. “Rapid color test identification system for screening of counterfeit fluoroquinolone”. J Chem. 2009. 6(2):377-384.

[20] A. Weaver, H. Reiser, T. Barstis, M. Benvenuti, D. Ghosh, M. Hunckler, B. Joy, L. Koenig, K. Raddell, M. Lieberman. “Paper analytical devices for fast field screening of beta lactam antibiotics and antituberculosis pharmaceuticals. Analytical chemistry”. Anal Chem. 2013. 85(13):6453-6460.

[21] H. Pan, W. Ba-Thein. “Diagnostic accuracy of Global Pharma Health Fund Minilab™ in assessing pharmacopoeial quality of antimicrobials”. Am J Trop Med Hyg. 2018. 98(1):344-348.

[22] F. Khuluza, S. Kigera, L. Heide. “Low prevalence of substandard and falsified antimalarial and antibiotic medicines in public and faith-based health facilities of southern Malawi”. Am J Trop Med Hyg. 2017. 96(5):1124-1135.

[23] M. Gaudiano, A. Di Maggio, E. Antoniella, L. Valvo, P. Bertocchi, L. Manna, M. Bartolomei, S. Alimonti, A. Rodomonte. “An LC method for the simultaneous screening of some common counterfeit and sub-standard antibiotics: validation and uncertainty estimation”. J Pharmaceut Biomed. 2008. 48(2):303-309.

[24] S. Schäfermann, E. Wemakor, C. Hauk, L. Heide, “Quality of medicines in southern Togo: Investigation of antibiotics and of medicines for non-communicable diseases from pharmacies and informal vendors”. PloS one. 2018. 13(11):e0207911.

[25] N. Tshilombo, P. Hamuli, J. Mbinze, V. Habyalimana, D. Kalenda, D. Mavungu, P. Mwamba, P. Hubert. “Investigation of the Quality of Antibiotics-Based Amoxicillin for Monitoring of Some Different Medicine Markets of Democratic Republic of Congo”. Am J Anal Chem. 2018. 9(08):366-385.

[26] J. Mbinze, P. Lebrun, B. Debrus, A. Dispas, N. Kalenda, J. Mbay, R. Marini. “Application of an innovative design space optimization strategy to the development of liquid chromatographic methods to combat potentially counterfeit nonsteroidal anti-inflammatory drugs”. J Chromatogr A. 2012. 1263:113-124.

[27] S. Bekoe, S. Bak, E. Björklund, K. Krogh, N. Okine, R. Adosraku, B. Styrishave, M. Hansen. “Determination of thirteen antibiotics in drug products–A new LC-MS/MS tool for screening drug product quality”. Anal. Methods. 2014. 6(15):5847-5855.

[28] A. Solangi, S. Memon, M. Khuhawar, M. Bhanger. “Quantitative analysis of eight cephalosporin antibiotics in pharmaceutical products and urine by capillary zone electrophoresis”. Acta Chromatographica. 2007. 19:81.

[29] S. Assi, R. Watt, A. Moffat. “Assay of ciprofloxacin in intact and powdered tablets by near-infrared spectroscopy”. J Pharm Pharmacol. 2008.

[30] S. Assi, R. Watt, A. Moffat. “Identification of counterfeit medicines from the Internet and the World market using near-infrared spectroscopy”. Anal. Methods. 2011. 3(10):2231-6.

[31] T. Sakamoto, Y. Fujimaki, Y. Hiyama. “NIR spectroscopic investigation of two fluoroquinolones, levofloxacin and ofloxacin, and their tablets for qualitative identification of commercial products on the market”. Die Pharmazie. 2008. 63(9):628-32.

[32] H. Yang, B. Hu, X. Pan, S. Yan, Y. Feng, X. Zhang, L. Yin, C. Hu. “Deep belief network-based drug identification using near infrared spectroscopy”. J Innov Opt Heal Sci. 2017. 10(2):1630011.

[33] United States Pharmacopeia. United States Pharmacopoeial Convention. Inc, Rockville, MD. 2008.

[34] Near-infrared spectrophotometry in the British Pharmacopoeia. The British Pharmacopoeia Comission, Stationery Office, Norwich. 2010. A150-A154.

[35] R. Jee, Near-infrared spectroscopy in A. Moffat, M. Osselton, and B. Widdop. Clarke's Analysis of Drugs and Poisons. Pharmaceutical Press, London. 2004. 3rd ed. 346-357.

[36] K. Varmuza, P. Filzmoser. Introduction to multivariate statistical analysis in chemometrics. CRC press. 2016.

[37] R. Brereton. “Consequences of sample size, variable selection, and model validation and optimization, for predicting classification ability from analytical data”. TrAC. 2006. 25(11):1103-1111.

[38] A. Pomerantsev, O. Rodionova. “Concept and role of extreme objects in PCA/SIMCA”. J Chemom. 2014. 28(5):429-38.

[39] O. Rodionova, L. Houmøller, A. Pomerantsev, P. Geladi, J. Burger, V. Dorofeyev, A. Arzamastsev. “NIR spectrometry for counterfeit drug detection: a feasibility study”. Anal Chim Acta. 2005. 549(1-2):151-158.

[40] A. Moffat, S. Assi, R. Watt. “Identifying counterfeit medicines using near infrared spectroscopy”. J Near Infrared Spec. 2010. 18(1):1-5.

[41] D. Burns, E. Ciurczak. Handbook of Near-Infrared Spectroscopy. CRC Press. Taylor & Francis Group. Boca Raton. 2008. pp:631-645

[42] S. Kovacs, S. Hawes, S. Maley, E. Mosites, L. Wong, A. Stergachis. “Technologies for detecting falsified and substandard drugs in low and middle-income countries”. PloS one. 2014. 9(3), p.e90601.

[43] O. Rodionova, K. Balyklova, A. Titova, A.Pomerantsev. “Quantitative risk assessment in classification of drugs with identical API content”. J.Pharm.Biomed.Anal. 2014. 89:186–192.

List of tables

Table 1. Details of the antibiotics used in the study

AN	API	Dose (mg)	B/G	Manufacturing place	Source	Formulation type
AMC1	amoxicillin trihydrate/ clavulanic acid	500/ 125	B	UK	Lebanon/ Community pharmacy	tablet
AMC2	amoxicillin trihydrate/ clavulanic acid	500/ 125	G	Lebanon	Lebanon/ Humanitarian aid	tablet
AMC3	amoxicillin trihydrate/ clavulanic acid	500/ 125	G	Spain	Lebanon/ Humanitarian aid	tablet
AZ1	azithromycin dihydrate	250	G	UK	UK/ wholesaler	tablet
AZ2	azithromycin dihydrate	250	B	Italy	Italy/ wholesaler	tablet
AZ3	azithromycin dihydrate	250	B	Italy	Italy/ wholesaler	capsule
AZ4	azithromycin dihydrate	250	B	Italy	Italy/ wholesaler	capsule
CIP1	ciprofloxacin hydrochloride	500	B	Germany	UK/ wholesaler	tablet
CIP2	ciprofloxacin hydrochloride	500	B	Germany	UK/ wholesaler	tablet
CIP3	ciprofloxacin hydrochloride	750	B	Germany	UK/ online pharmacy	tablet
CIP4	ciprofloxacin hydrochloride	500	B	Germany	UK/ online pharmacy	tablet
CIP5	ciprofloxacin hydrochloride	250	B	Germany	UK/ online pharmacy	tablet
CIP6	ciprofloxacin hydrochloride	500	G	Ghana	Ghana/ street market	tablet
CIP7	ciprofloxacin hydrochloride	500	G	UAE	Saudi Arabia/ hospital pharmacy	tablet
CIP8	ciprofloxacin hydrochloride	500	G	India	UK/ wholesaler	tablet
CIP9	ciprofloxacin hydrochloride	500	G	UK	UK/ community pharmacy	tablet
CIP10	ciprofloxacin hydrochloride	250	G	India	Lebanon/ Humanitarian aid	tablet
CIP11	ciprofloxacin hydrochloride	500	G	UK	UK/ community pharmacy	tablet

CIP12	ciprofloxacin hydrochloride	500	G	UK	UK/ community pharmacy	tablet
DOX1	doxycycline hydrochloride	100	G	Jordan	Lebanon/ Humanitarian aid	capsule
DOX2	doxycycline hydrochloride	100	G	Austria	Lebanon/ community pharmacy	capsule
OFL1	ofloxacin	200	G	UK	UK/ wholesaler	tablet
OFL2	ofloxacin	200	B	France	UK/ wholesaler	tablet

AM: Amoxicillin, API: Active pharmaceutical ingredient, AZ: Azithromycin, B: Branded, G: Generic, CIP: Ciprofloxacin, DOX: Doxycycline, OFL: Ofloxacin, UAE: United Arab Emirates.

Table 2. List of excipients studied in the investigated antibiotics

Excipient/AN	AMC 1	AMC 2	AMC 3	AZ 1	AZ 2	AZ 3	AZ 4	CIP 1	CIP 2	CIP 3	CIP 4	CIP 5	CIP 6	CIP 7	CIP 8	CIP 9	CIP1 0	CIP1 1	CIP1 2	DOX 1	DOX 2	OFL 1	OFL 2
Butyl hydroxy toluene				■																			
Calcium hydrogen phosphate				■																			
Carmellose NS300																							■
Colloidal silicon dioxide	■	■	■	■				■	■	■	■	■		■	■	■						■	
Croscarmellose sodium		■	■													■						■	
Crospovidone		■						■	■	■	■	■		■		■		■	■				
Dimethicone	■																						
Ethanol 96%														■									
Ethyl cellulose		■																					
Gelatin					■	■	■																
Hyprolose																							■
Hypromellose	■	■	■					■	■	■	■	■		■	■	■		■	■			■	■
Lactose monohydrate					■	■	■											■	■			■	■
Macrogol 3000																						■	
Macrogol 4000	■							■	■	■	■	■		■	■	■		■	■				
Macrogol 6000	■																						
Macrogol 8000																							■
Maize starch					■	■	■	■	■	■	■	■			■							■	■
MCC	■	■	■	■				■	■	■	■	■		■	■	■							
MgS	■	■	■	■	■	■	■	■	■	■	■	■		■	■	■						■	■
Propylene glycol			■																				
Sodium citrate																							
Sodium lauryl sulfate			■	■	■	■	■																
Sodium starch glycolate	■		■											■	■			■	■				

Sodium stearyl fumarate																		■	■			
Talc		■	■																			■
Titanium dioxide	■	■	■		■	■	■	■	■	■	■		■	■	■		■	■			■	■
Triacetin																					■	
Triethyl citrate		■																				
Total number of excipients	9	10	10	6	6	6	6	8	8	8	8	8	NR	9	8	8	NR	7	7	NR	NR	9	9

AMC: amoxiciilin/clavulanic acid; AN: antibiotic number; AZ: azithromycin; CIP: ciprofloxacin, DOX: doxycycline; MgS: magnesium stearate; MCC: microcrystalline cellulose; NR: not reported; OFL: ofloxacin

Table 3. Inter-material distances explained by the SIMCA models.

Material	Doxycycline	Ofloxacin	Ciprofloxacin	Amoxycillin	Azithromycin
Doxycycline	-	24	30.5	28.2	28.7
Ofloxacin	24	-	28.1	19.3	16.3
Ciprofloxacin	30.5	28.1	-	25.4	34.5
Amoxicillin	28.2	19.3	25.4	-	23.5
Azithromycin	28.7	16.3	34.5	23.5	-

Figure captions

Figure 1. MSC-D1 NIR spectra of (a) amoxicillin/clavulanic acid; (b) azithromycin; (c) ciprofloxacin; (d) doxycycline; (e) ofloxacin branded antibiotic products and their main excipients including (f) lactose; (g) maize starch; (h) MCC; and (i) talc measured using the PerkinElmer Spectrum Two N FT-NIR instrument equipped with NIRM.

Figure 2. (a) Two-dimensional and (b) three-dimensional PCA scores plots of the MSC-D1 NIR spectra of branded antibiotic products of amoxicillin/clavulanic acid (blue), azithromycin (red), ciprofloxacin (green), doxycycline (cyan), and ofloxacin (black) measured using the PerkinElmer Spectrum Two N FT-NIR instrument equipped with NIRM.

Figure 3. PC1 loading plot of the different brands that contributed to 51.2% of the variance among the data.

Figure 4. PCA scores plots of the MSC-D1 spectra of antibiotics products including (a) amoxicillin/clavulanic acid, (b) azithromycin, (c) doxycycline, and (d) ofloxacin measured using the PerkinElmer Spectrum Two N FT-NIR instrument equipped with NIRM. The first three PCA scores plots were two-dimensional whereas the latter score plot was three-dimensional.

Figure 5. PCA scores plot of the MSC-D1 NIR spectra of branded (blue) and generic (red) ciprofloxacin batches measured using the PerkinElmer Spectrum Two N FT-NIR instrument equipped with NIRM.

Figure 6. SIMCA models of the MSC-D1 spectra of antibiotics products including (a) amoxicillin/clavulanic acid, (b) azithromycin, (c) ciprofloxacin, (d) doxycycline, and (e) ofloxacin measured using the PerkinElmer Spectrum Two N FT-NIR instrument equipped with NIRM.

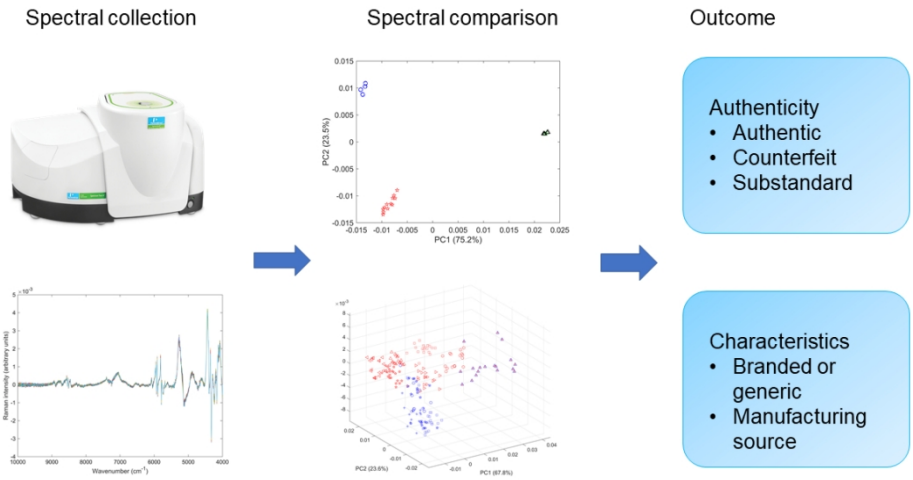

338x190mm (96 x 96 DPI)

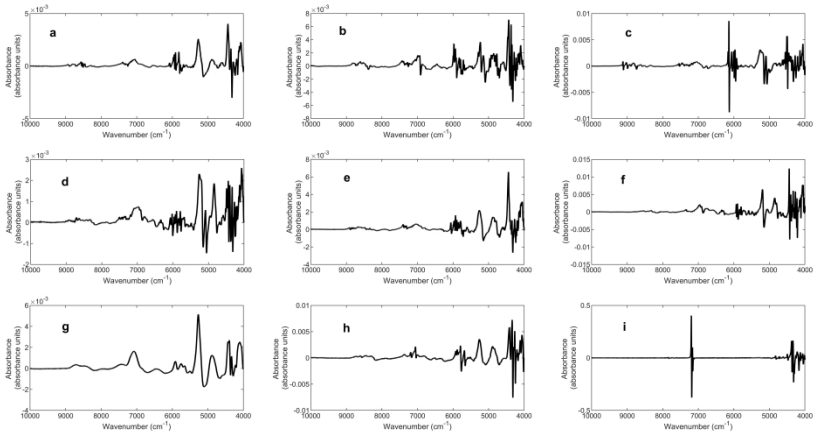

260x126mm (600 x 600 DPI)

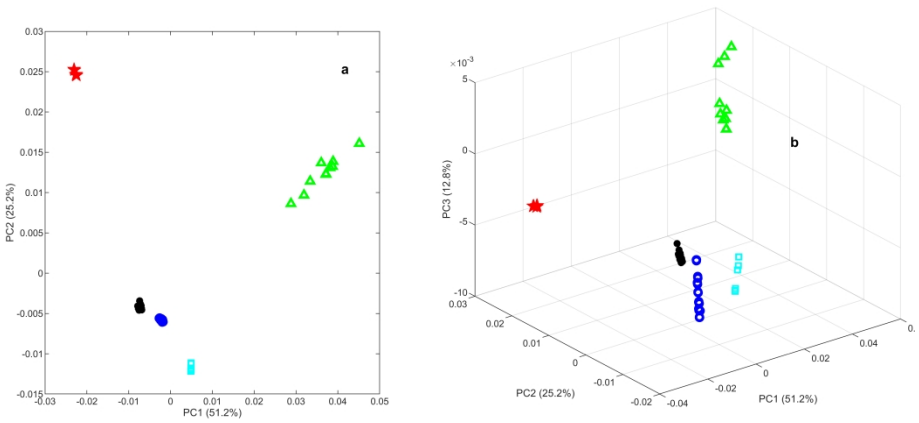

Figure 2. PCA scores plot of the MSC-D1 spectra of branded antibiotic products of amoxicillin/clavulanic acid (blue), azithromycin (red), ciprofloxacin (green), doxycycline (cyan) and ofloxacin (black) measured using the PerkinElmer Spectrum Two N FT-NIR instrument equipped with NIRM.

303x134mm (600 x 600 DPI)

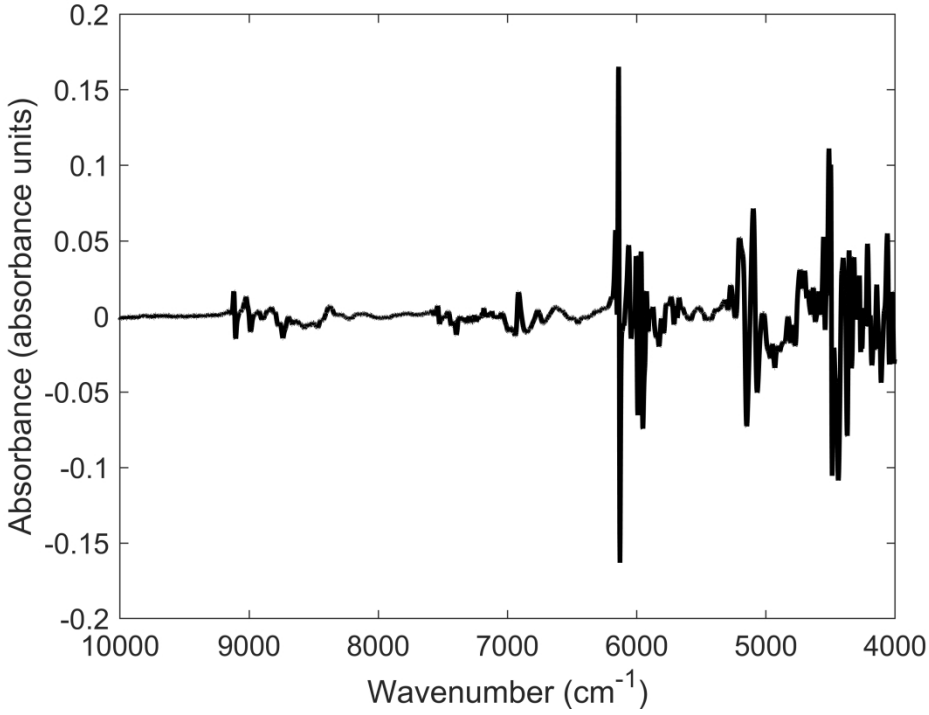

Figure 3. PC1 loading plot of the different brands that contributed to 51.2% of the variance among the data.

148x111mm (600 x 600 DPI)

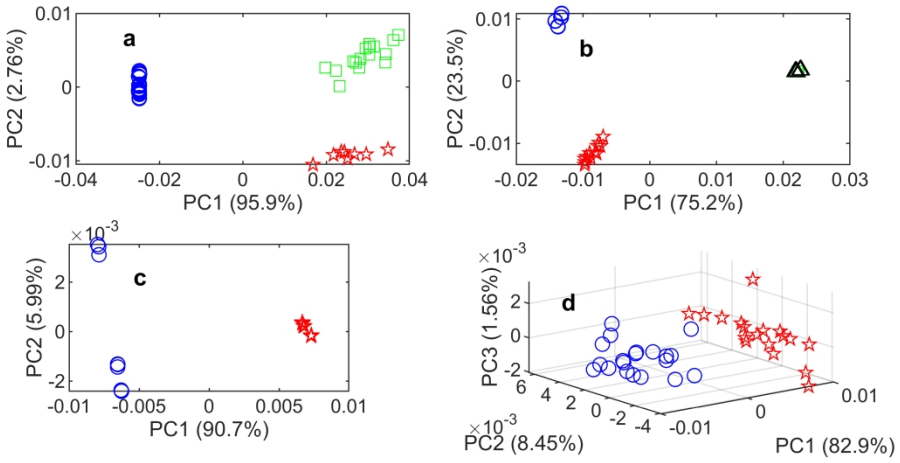

Figure 4. PCA scores plots of the MSC-D1 spectra of antibiotics products including (a) amoxicillin/clavulanic acid, (b) azithromycin, (c) doxycycline and (d) ofloxacin measured using the PerkinElmer Spectrum Two N FT-NIR instrument equipped with NIRM.

148x111mm (600 x 600 DPI)

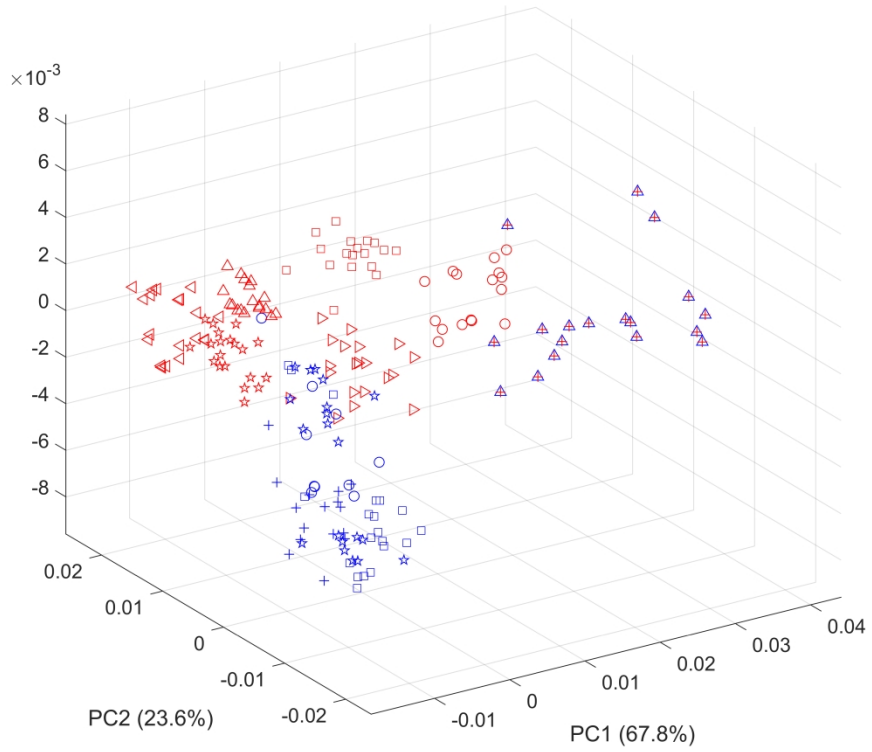

Figure 5. PCA scores plot of the MSC-D1 NIR spectra of branded (blue) and generic (red) ciprofloxacin batches measured using the PerkinElmer Spectrum Two N FT-NIR instrument equipped with NIRM.

212x186mm (600 x 600 DPI)

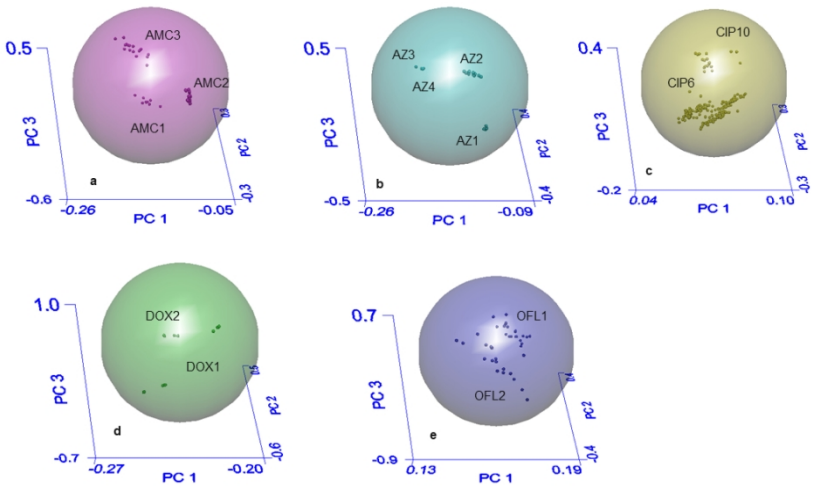

Figure 6. SIMCA models of the MSC-D1 spectra of antibiotics products including (a) amoxicillin/clavulanic acid, (b) azithromycin, (c) ciprofloxacin, (d) doxycycline and (e) ofloxacin measured using the PerkinElmer Spectrum Two N FT-NIR instrument equipped with NIRM.

338x190mm (96 x 96 DPI)

Appendix A PCA loading plots of the antibiotic products

A1. List of excipients present in the products:

Butyl hydroxyl toluene; calcium hydroxyl toluene; carmellose NS300; colloidal silicon dioxide; croscarmellose sodium; crospovidone; dimethicone; ethanol 96%; ethyl cellulose; gelatin; hyprolose; hypromellose; lactose monohydrate; macrogol 3000; macrogol 4000; macrogol 6000; macrogol 8000; maize starch; MCC; MgS; propylene glycol; sodium citrate; sodium lauryl sulfate; sodium starch glycolate; sodium stearyl fumarate; talc; titanium dioxide; triacetin; triethyl citrate and titanium dioxide.

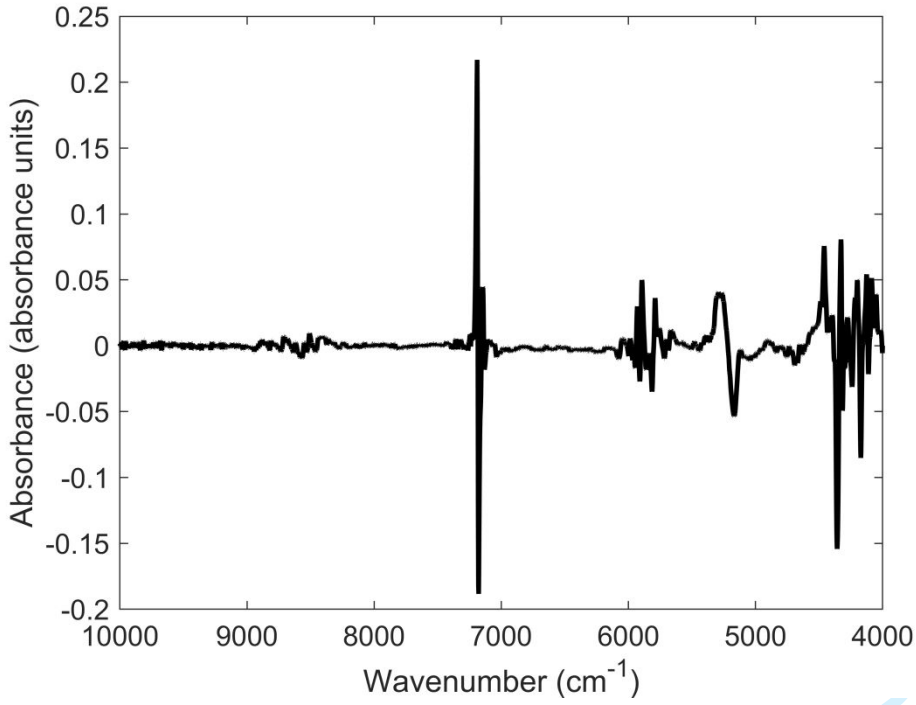

Figure A1. PC1 loading plot of the PCA of the MSC-D1 NIR spectra of AMC products that contributed to 95.9% of the variance among the data.

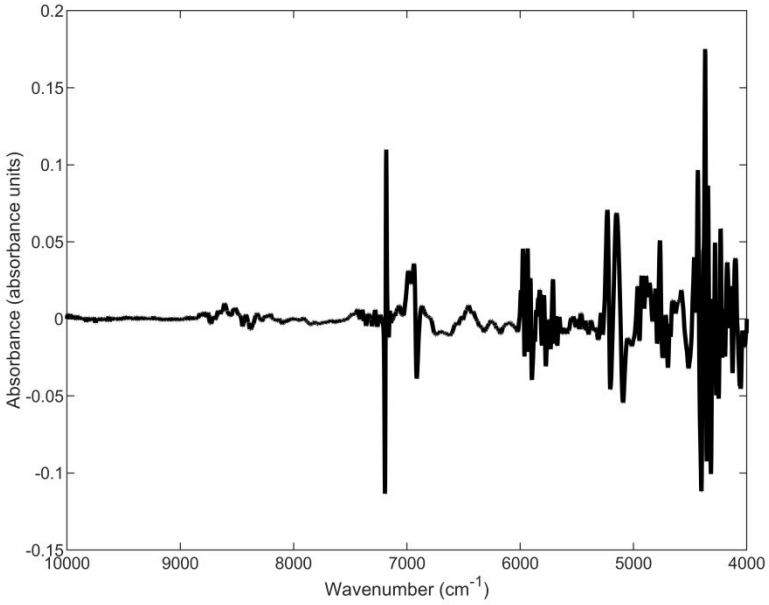

Figure A2. PC1 loading plot of the PCA of the MSC-D1 NIR spectra of AZ products that contributed to 75.2% of the variance among the data.

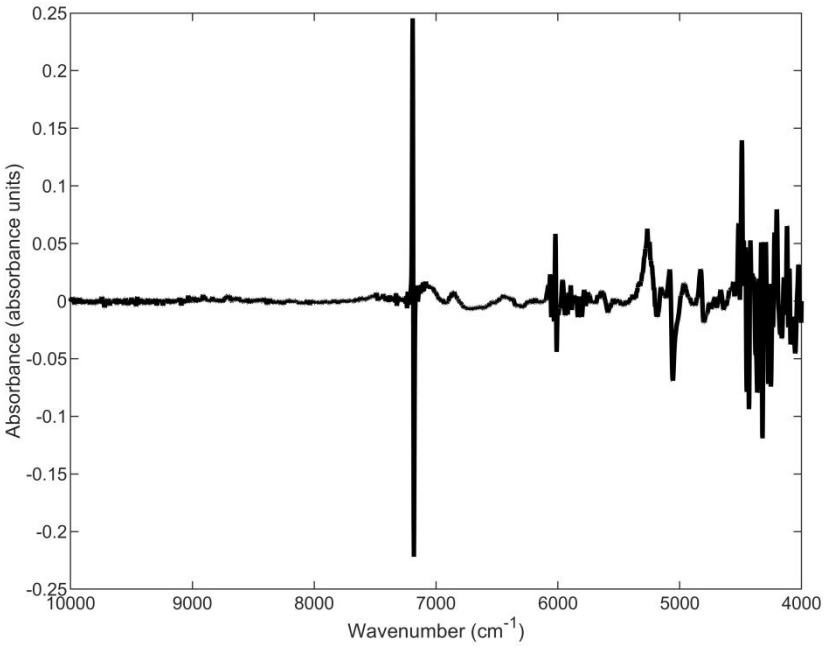

Figure A3. PC1 loading plot of the PCA of the MSC-D1 NIR spectra of DOX products that contributed to 90.7% of the variance among the data.

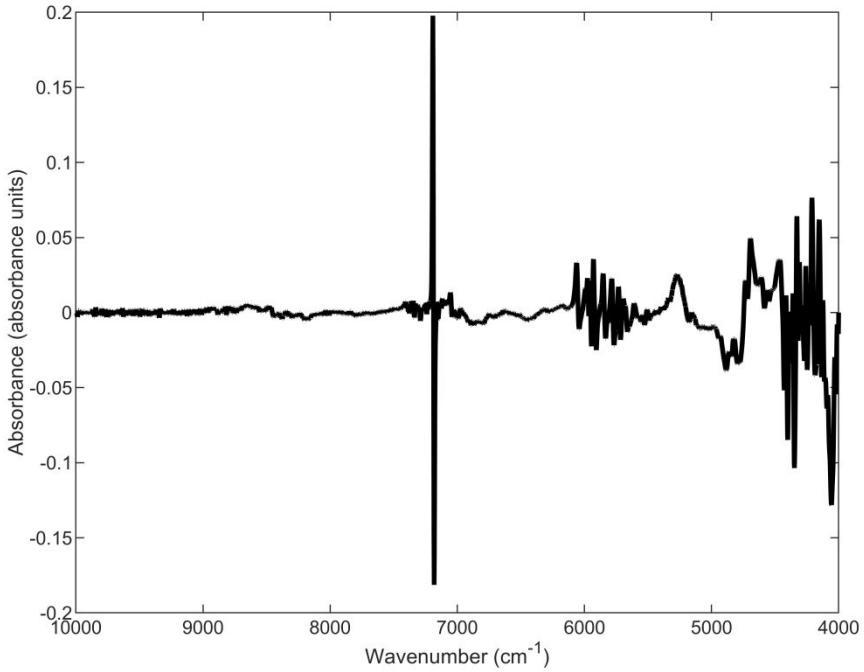

Figure A4. PC1 loading plot of the PCA of the MSC-D1 NIR spectra of OFL products that contributed to 82.9% of the variance among the data.

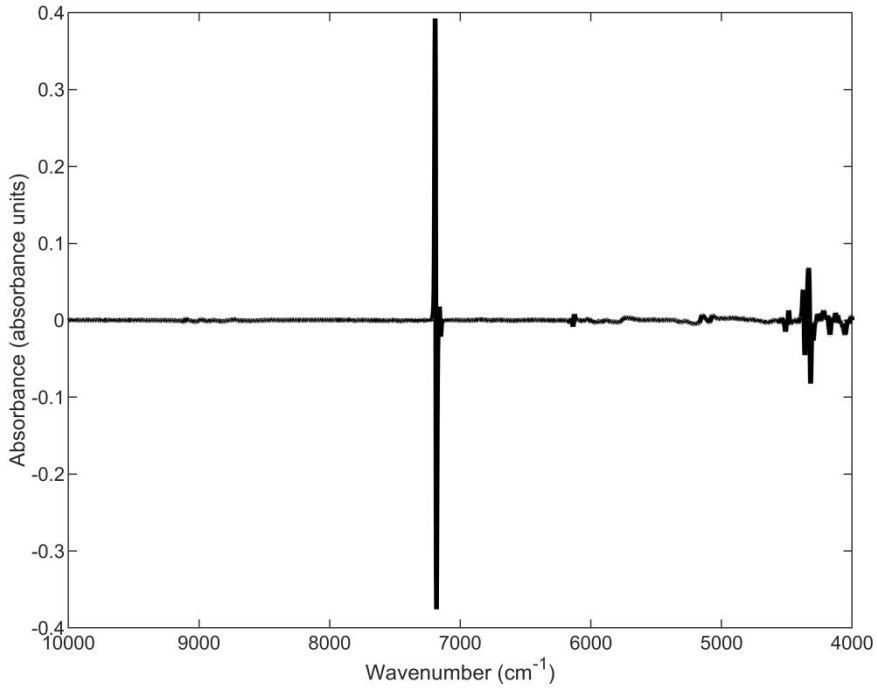

Figure A5. PC1 loading plot of the PCA of the MSC-D1 NIR spectra of CIP products that contributed to 67.8% of the variance among the data.

Appendix B NIR spectra of antibiotic products, APIs and common excipients present in products

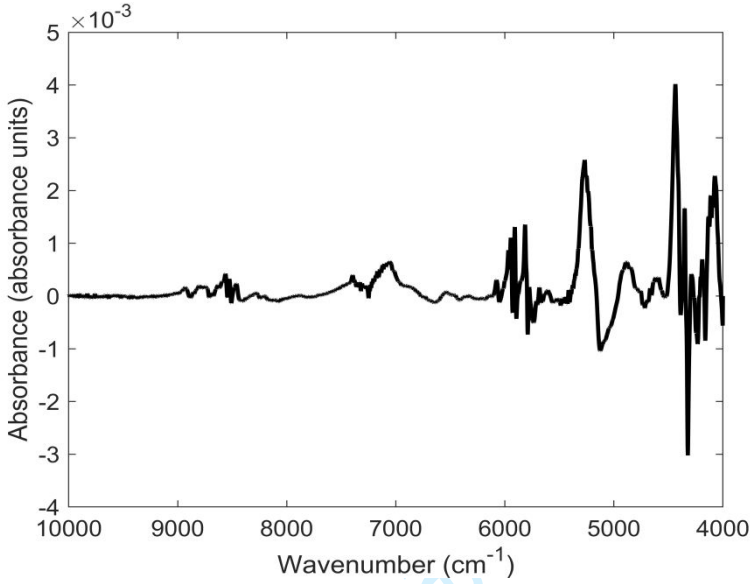

Figure B1. MSC-D1 NIR spectrum of AMC1 products measured using the Perkin Elmer Spectrum Two FT-NIR instrument equipped with NIRM.

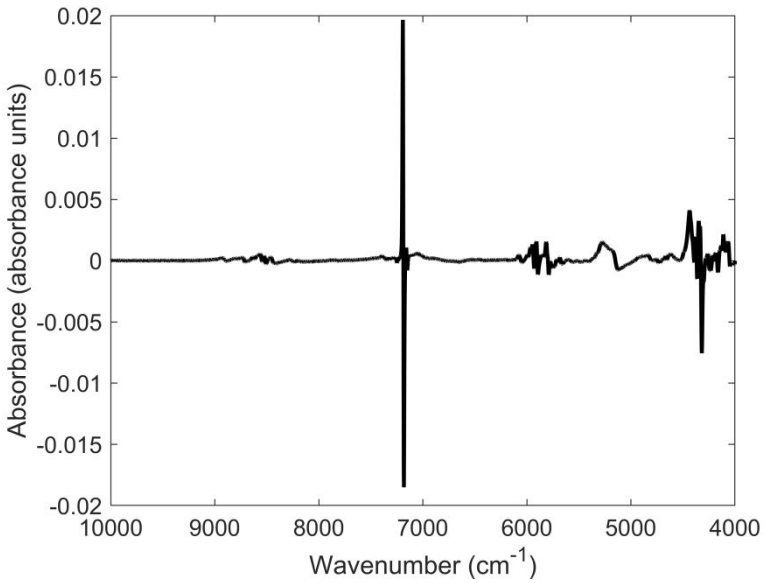

Figure B2. MSC-D1 NIR spectrum of AMC2 products measured using the Perkin Elmer Spectrum Two FT-NIR instrument equipped with NIRM.

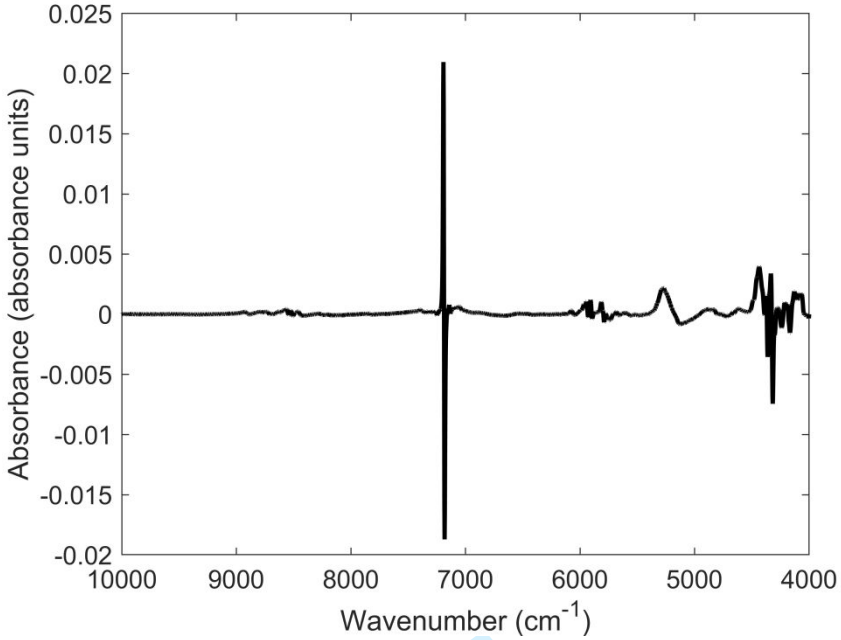

Figure B3. MSC-D1 NIR spectrum of AMC2 products measured using the Perkin Elmer Spectrum Two FT-NIR instrument equipped with NIRM.

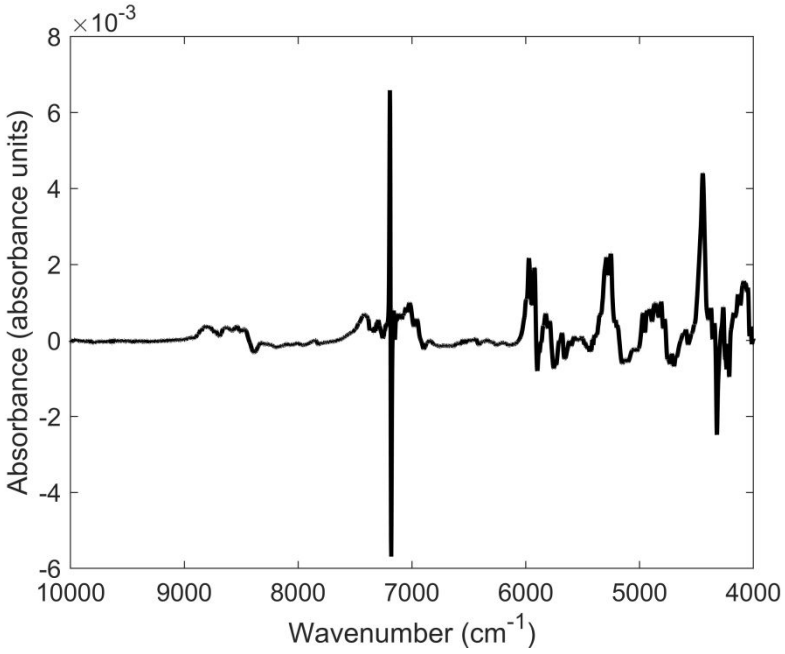

FigureB 4. MSC-D1 NIR spectrum of AZ1 products measured using the Perkin Elmer Spectrum Two FT-NIR instrument equipped with NIRM.

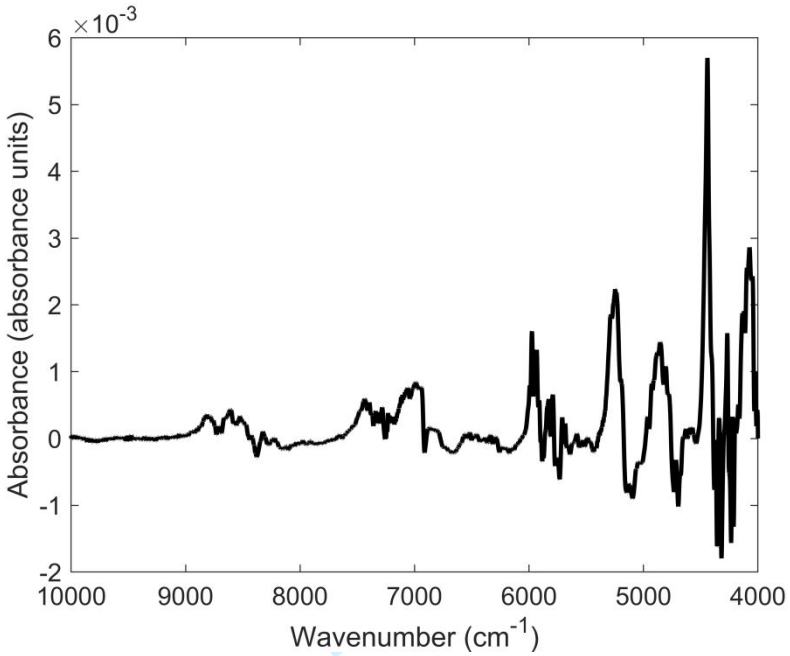

Figure B5. MSC-D1 NIR spectrum of AZ2 products measured using the Perkin Elmer Spectrum Two FT-NIR instrument equipped with NIRM.

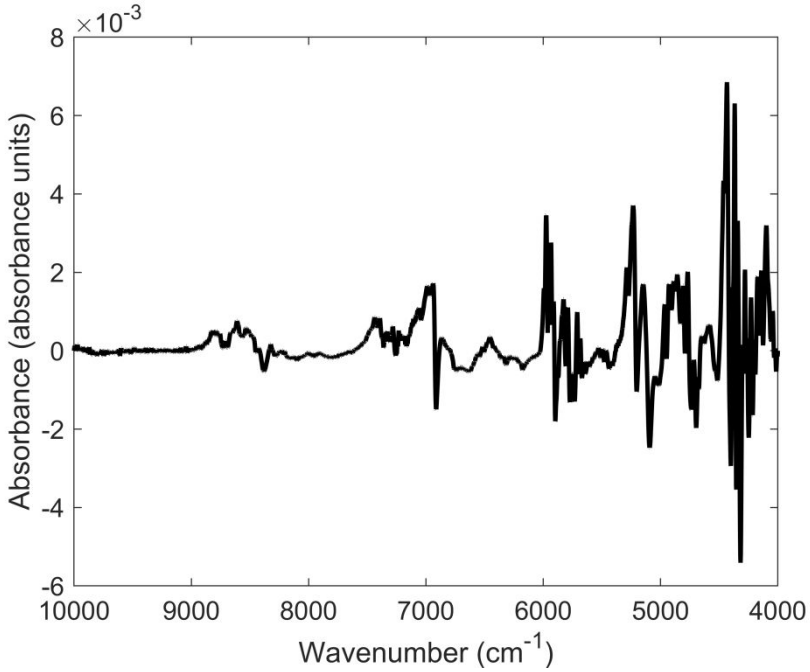

Figure B6. MSC-D1 NIR spectrum of AZ3 products measured using the Perkin Elmer Spectrum Two FT-NIR instrument equipped with NIRM.

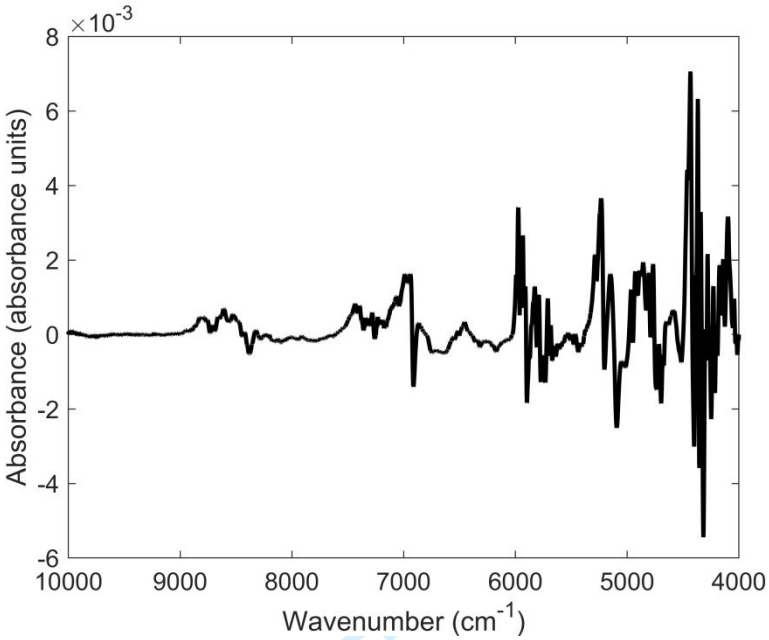

Figure B7. MSC-D1 NIR spectrum of AZ4 products measured using the Perkin Elmer Spectrum Two FT-NIR instrument equipped with NIRM.

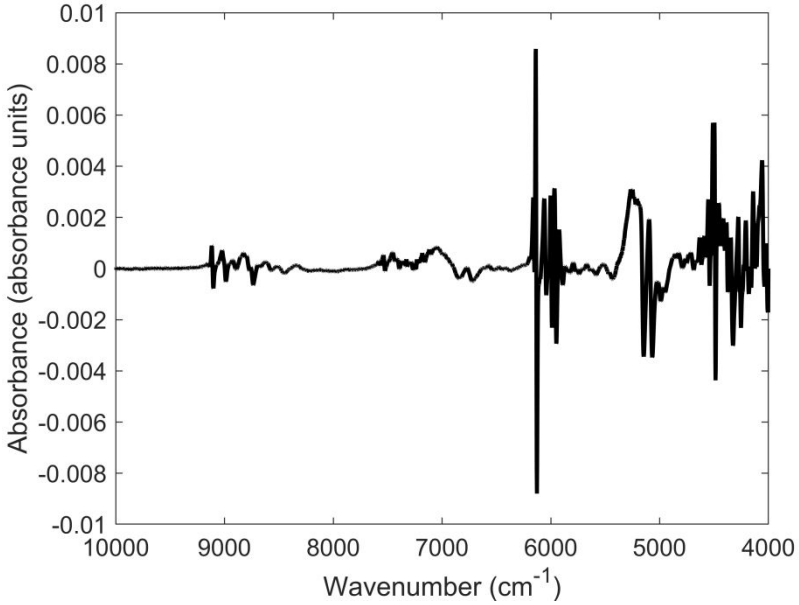

Figure B8. MSC-D1 NIR spectrum of CIP1 products measured using the Perkin Elmer Spectrum Two FT-NIR instrument equipped with NIRM.

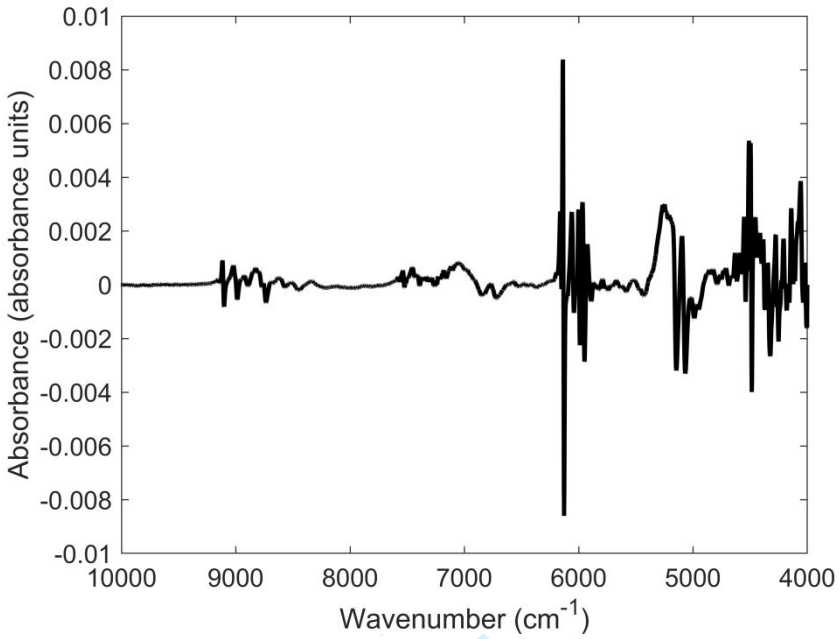

Figure B9. MSC-D1 NIR spectrum of CIP2 products measured using the Perkin Elmer Spectrum Two FT-NIR instrument equipped with NIRM.

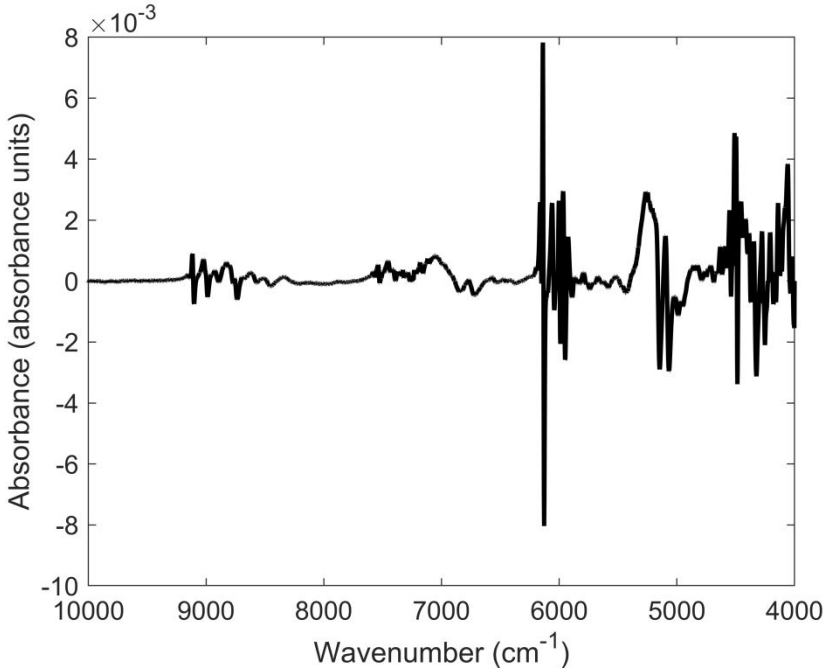

Figure B10. MSC-D1 NIR spectrum of CIP3 products measured using the Perkin Elmer Spectrum Two FT-NIR instrument equipped with NIRM.

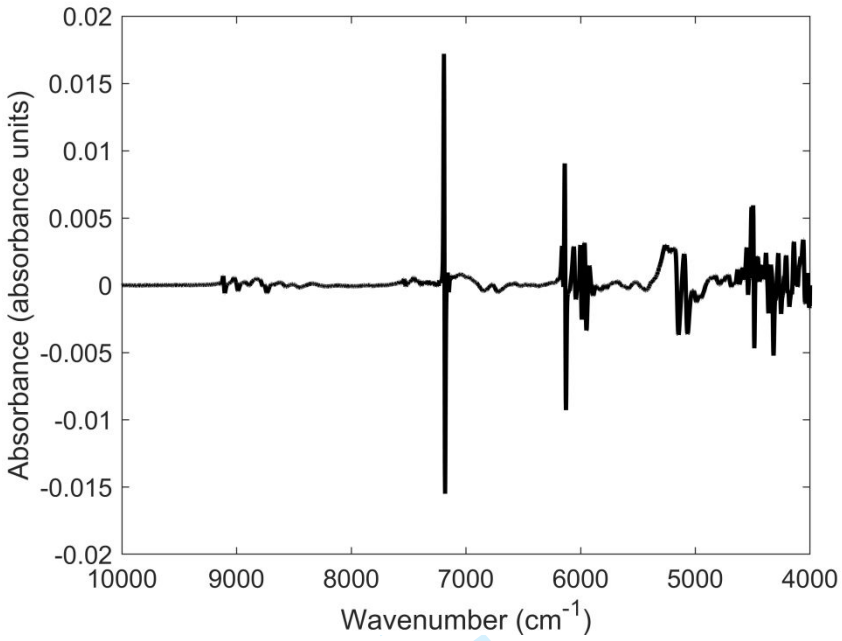

Figure B11. MSC-D1 NIR spectrum of CIP4 products measured using the Perkin Elmer Spectrum Two FT-NIR instrument equipped with NIRM.

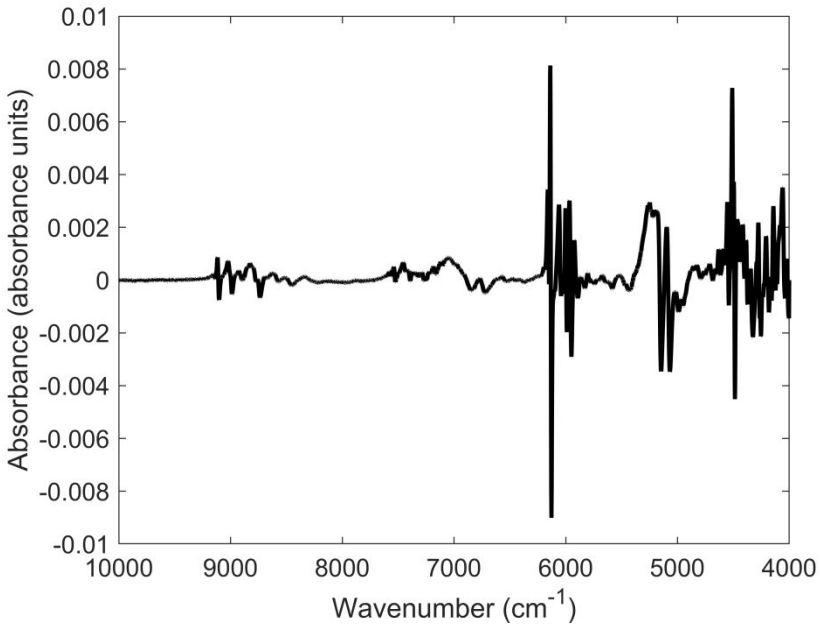

Figure B12. MSC-D1 NIR spectrum of CIP5 products measured using the Perkin Elmer Spectrum Two FT-NIR instrument equipped with NIRM.

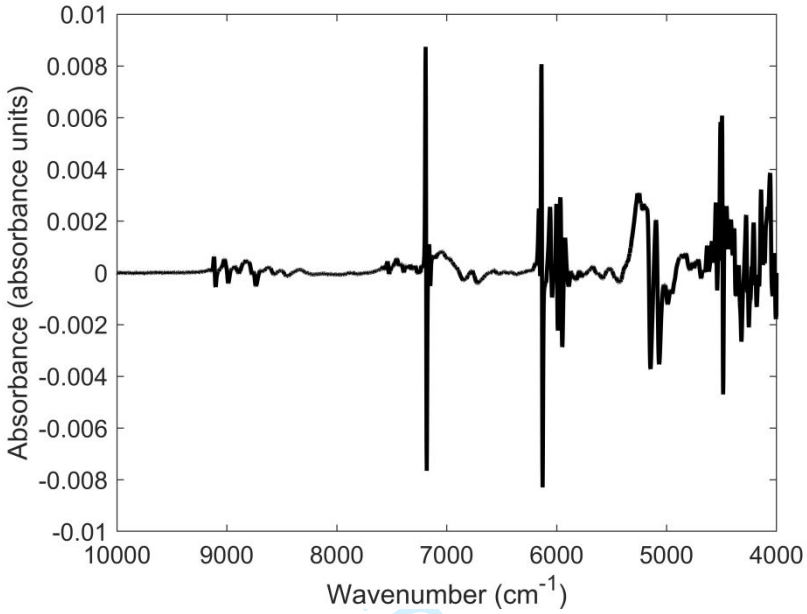

Figure B13. MSC-D1 NIR spectrum of CIP6 products measured using the Perkin Elmer Spectrum Two FT-NIR instrument equipped with NIRM.

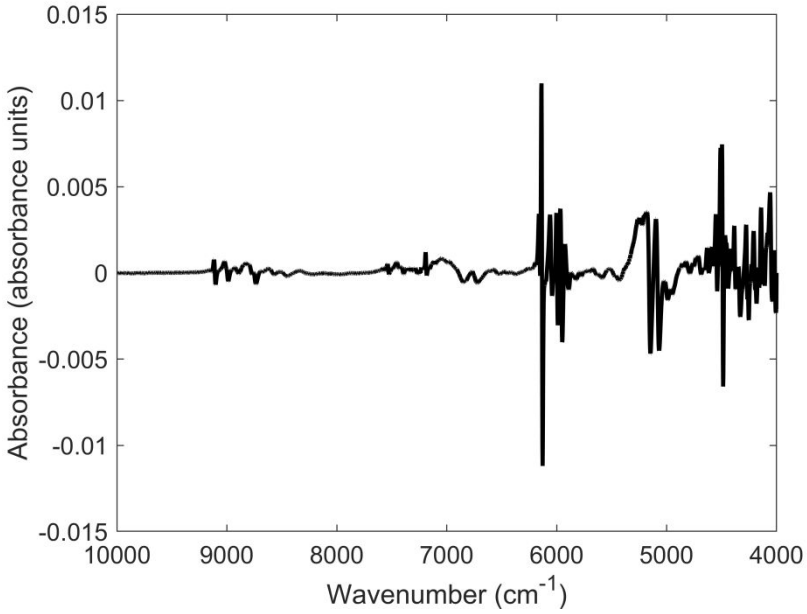

Figure B14. MSC-D1 NIR spectrum of CIP7 products measured using the Perkin Elmer Spectrum Two FT-NIR instrument equipped with NIRM.

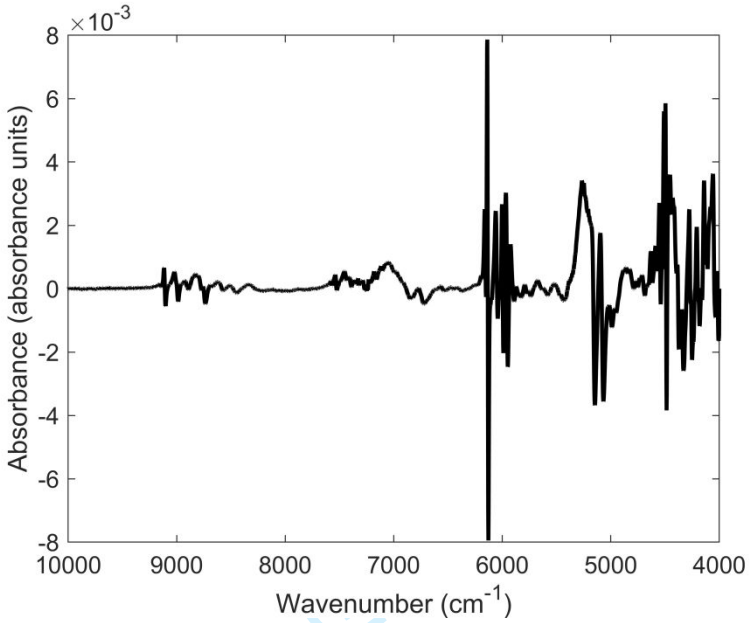

Figure B15. MSC-D1 NIR spectrum of CIP8 products measured using the Perkin Elmer Spectrum Two FT-NIR instrument equipped with NIRM.

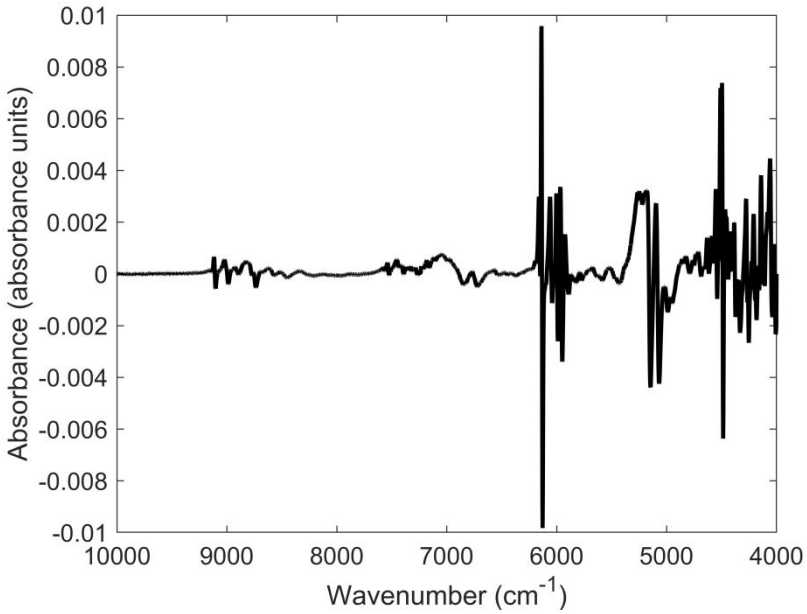

Figure B16. MSC-D1 NIR spectrum of CIP9 products measured using the Perkin Elmer Spectrum Two FT-NIR instrument equipped with NIRM.

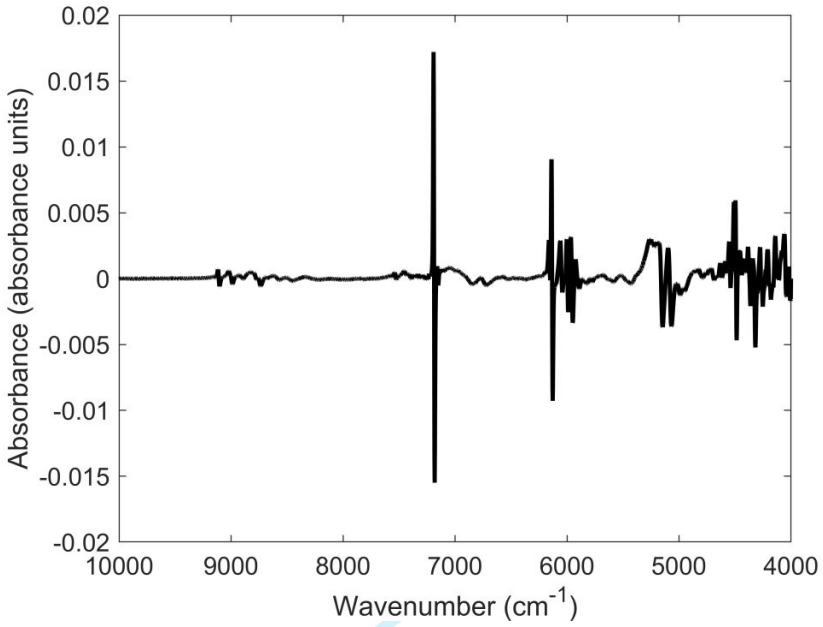

Figure B17. MSC-D1 NIR spectrum of CIP10 products measured using the Perkin Elmer Spectrum Two FT-NIR instrument equipped with NIRM.

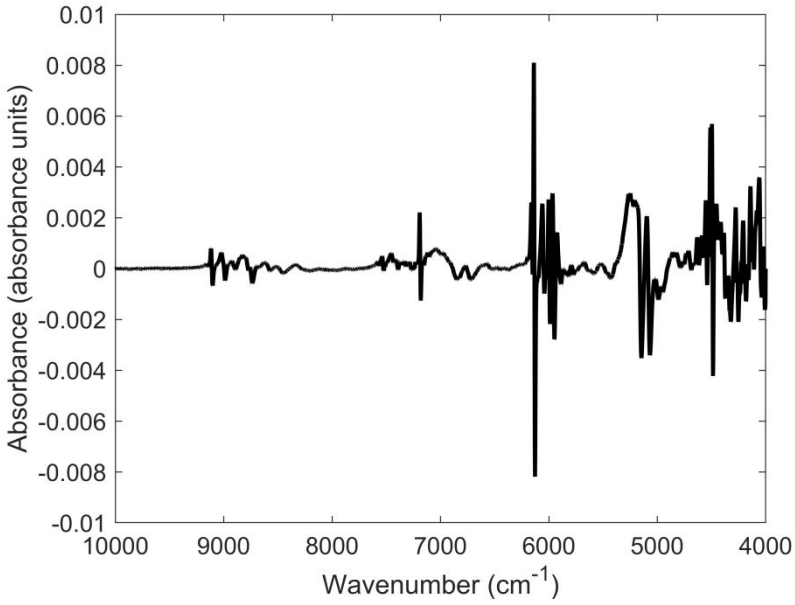

Figure B18. MSC-D1 NIR spectrum of CIP11 products measured using the Perkin Elmer Spectrum Two FT-NIR instrument equipped with NIRM.

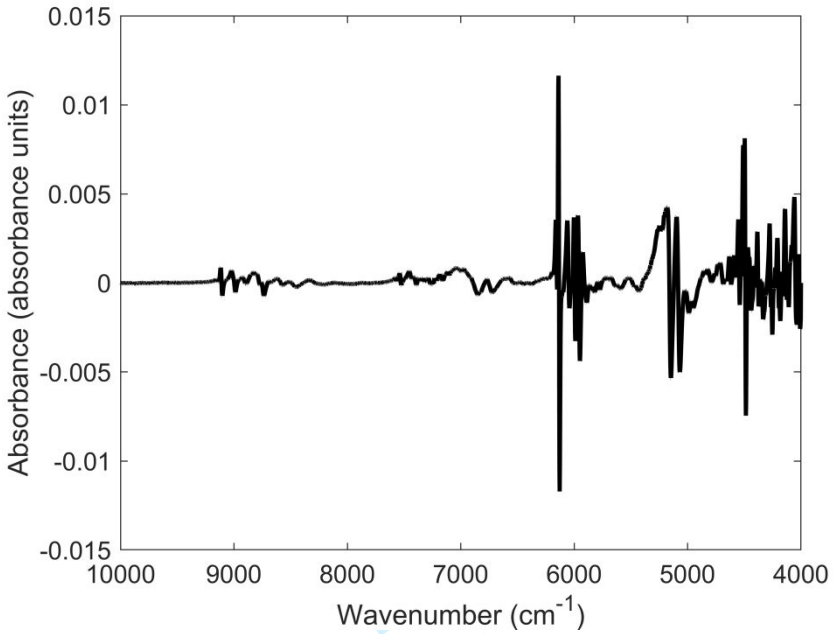

Figure B19. MSC-D1 NIR spectrum of CIP12 products measured using the Perkin Elmer Spectrum Two FT-NIR instrument equipped with NIRM.

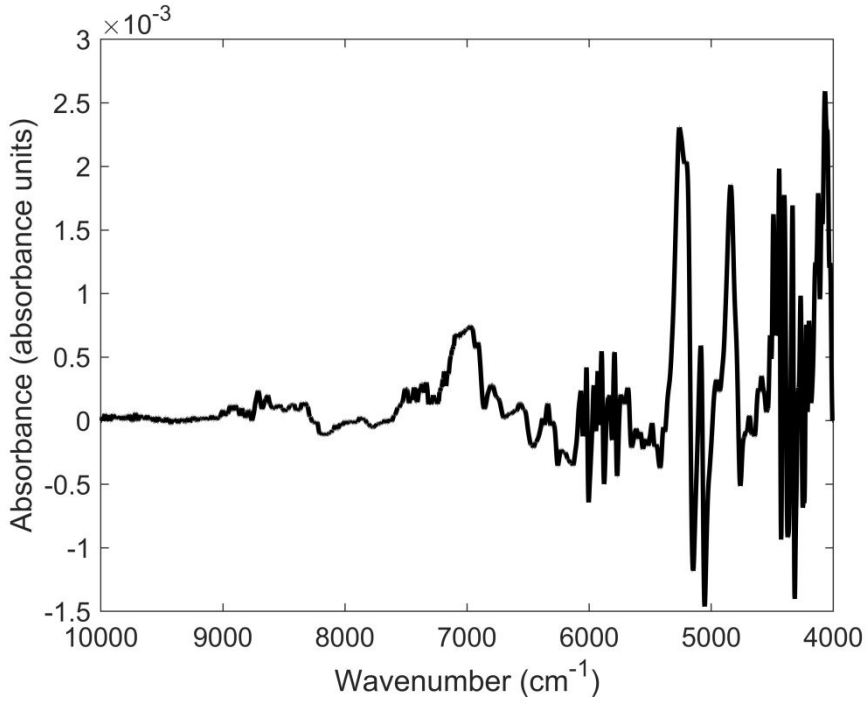

Figure B20. MSC-D1 NIR spectrum of DOX1 products measured using the Perkin Elmer Spectrum Two FT-NIR instrument equipped with NIRM.

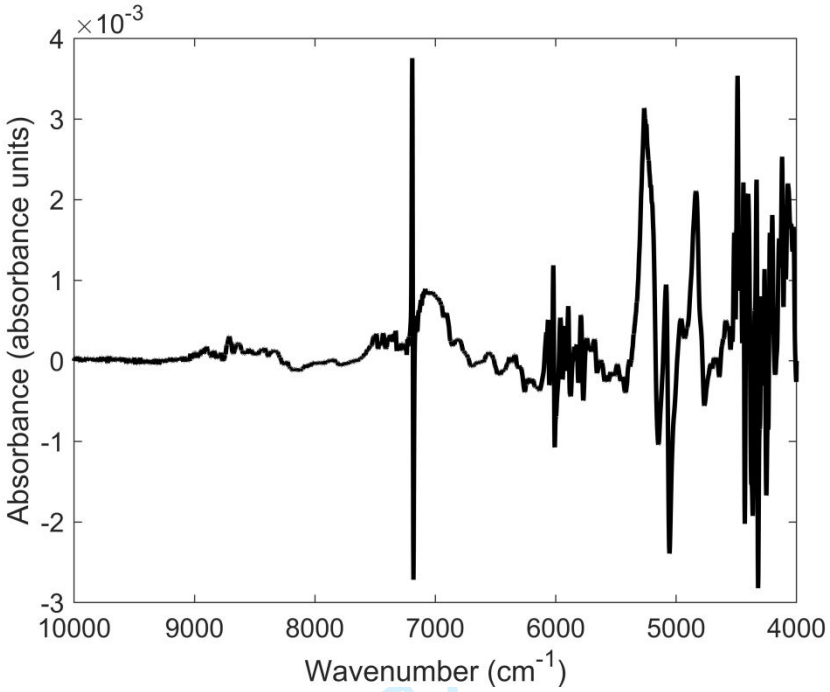

Figure B21. MSC-D1 NIR spectrum of DOX2 products measured using the Perkin Elmer Spectrum Two FT-NIR instrument equipped with NIRM.

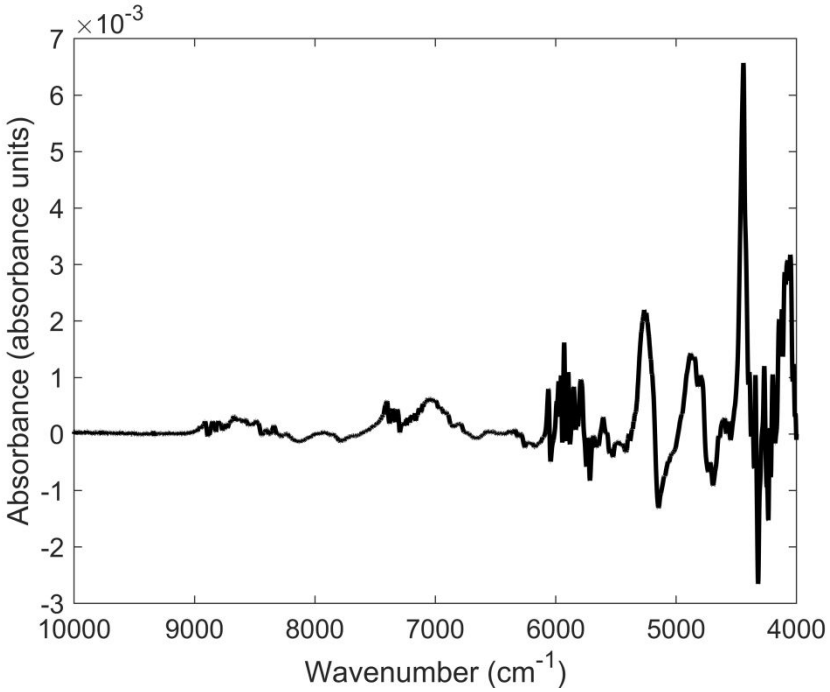

Figure B22. MSC-D1 NIR spectrum of OFL1 products measured using the Perkin Elmer Spectrum Two FT-NIR instrument equipped with NIRM.

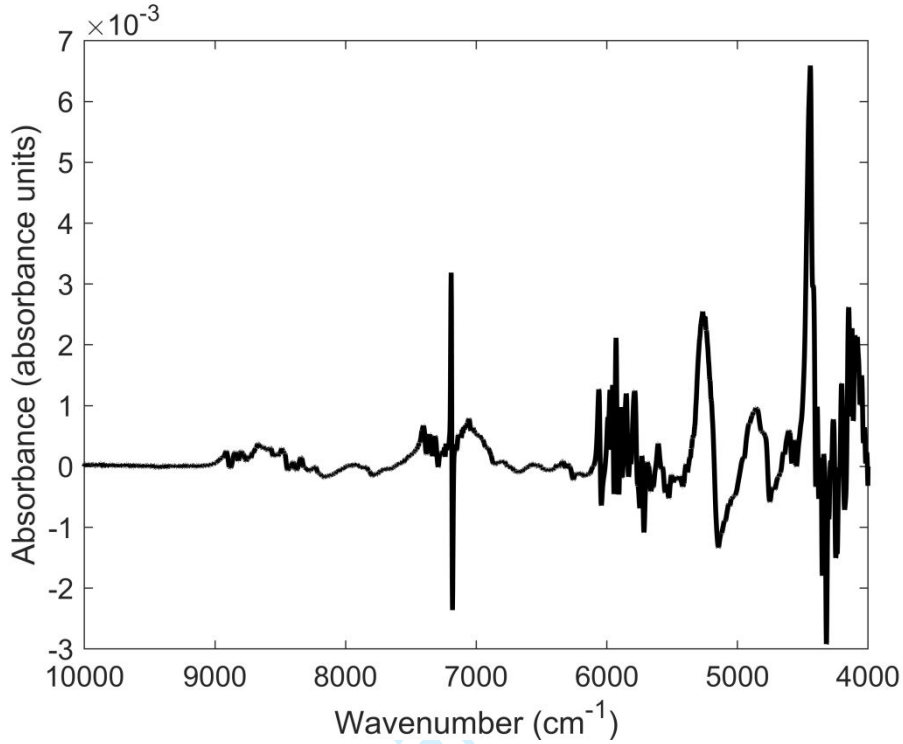

Figure B23. MSC-D1 NIR spectrum of OFL2 products measured using the Perkin Elmer Spectrum Two FT-NIR instrument equipped with NIRM.

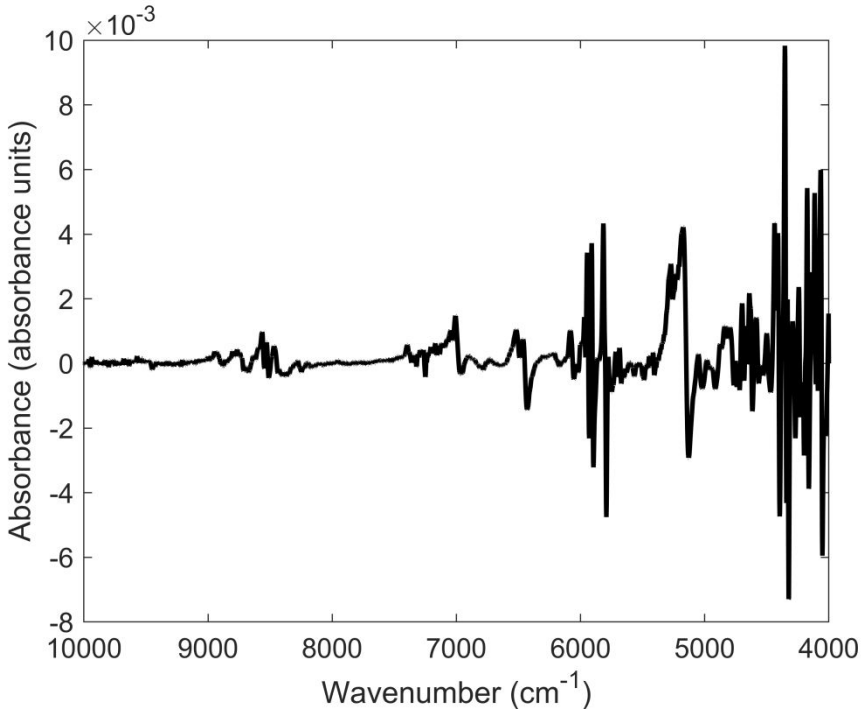

Figure B24. MSC-D1 NIR spectrum of amoxicillin trihydrate API measured using the Perkin Elmer Spectrum Two FT-NIR instrument equipped with NIRM.

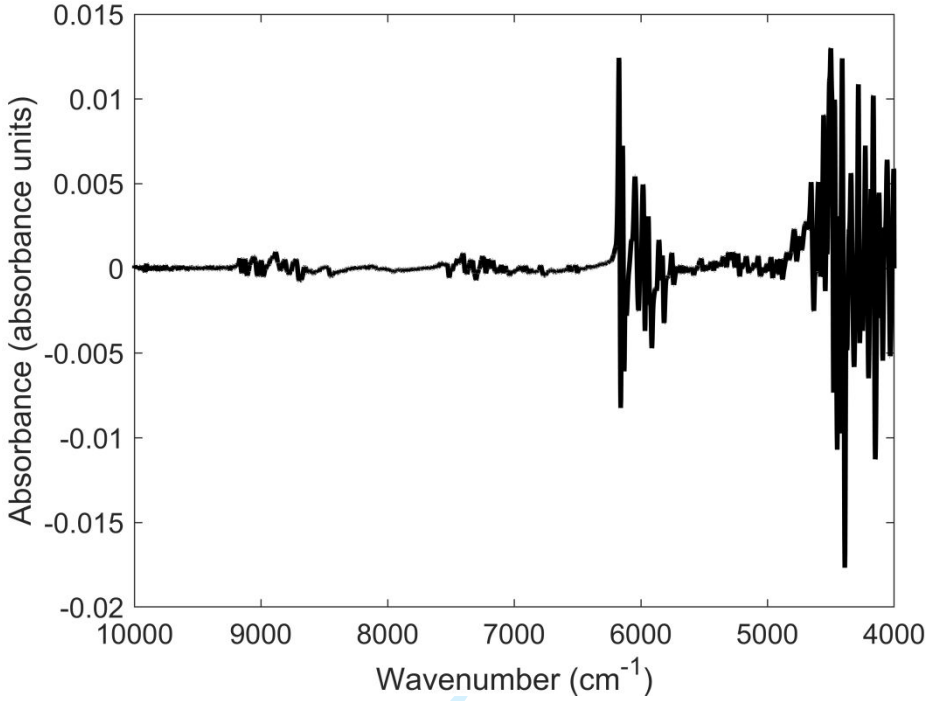

Figure B25. MSC-D1 NIR spectrum of ciprofloxacin hydrochloride API measured using the Perkin Elmer Spectrum Two FT-NIR instrument equipped with NIRM.

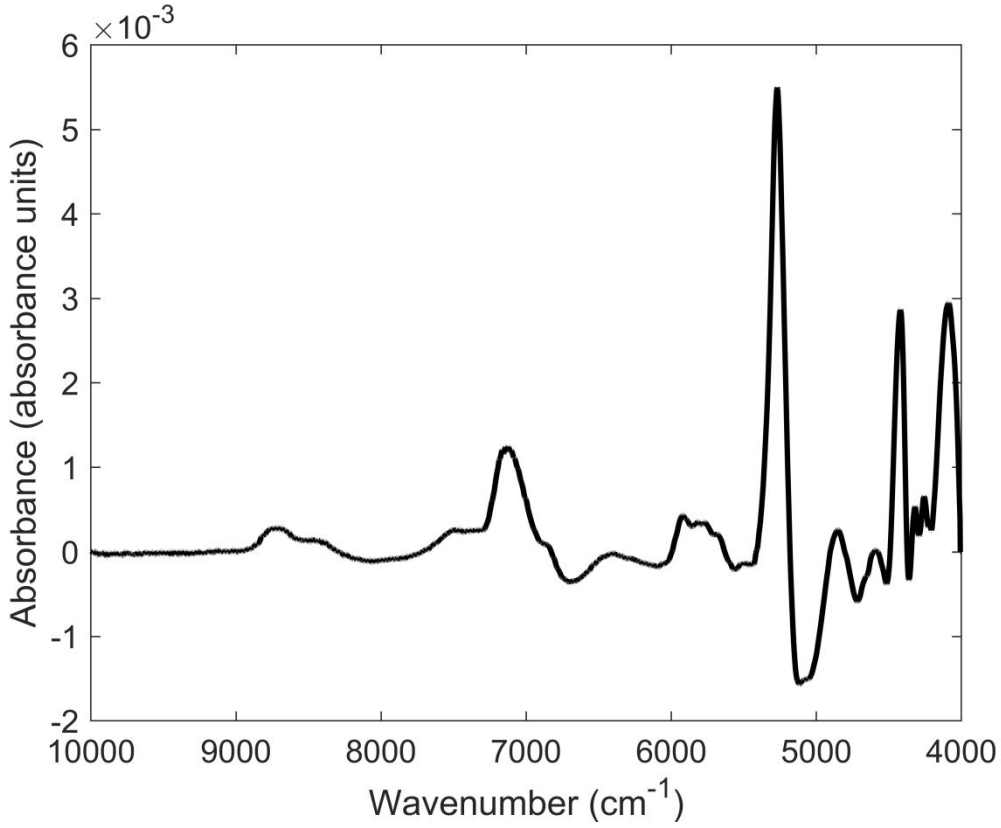

Figure B26. MSC-D1 NIR spectrum of croscarmellose sodium measured using the Perkin Elmer Spectrum Two FT-NIR instrument equipped with NIRM.

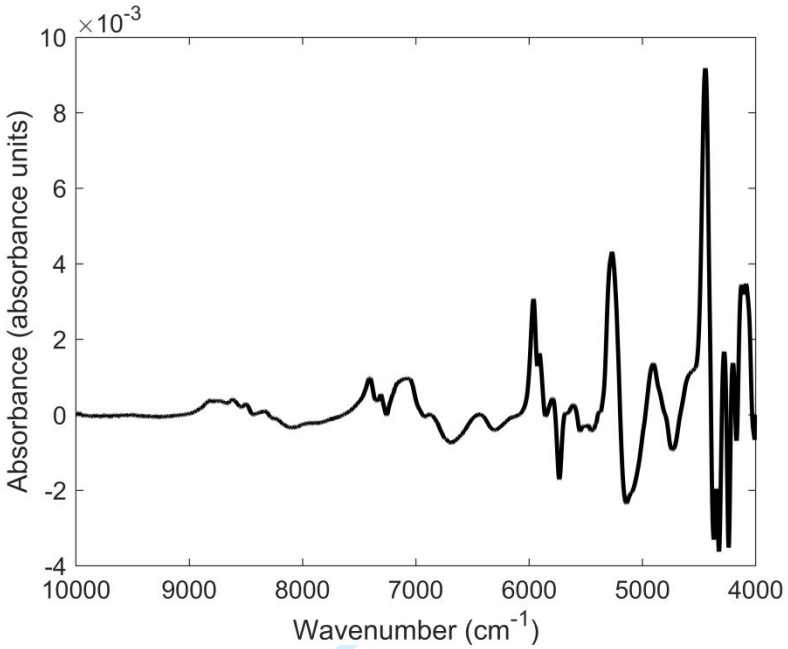

Figure B27. MSC-D1 NIR spectrum of hydroxyl propyl methyl cellulose measured using the Perkin Elmer Spectrum Two FT-NIR instrument equipped with NIRM.

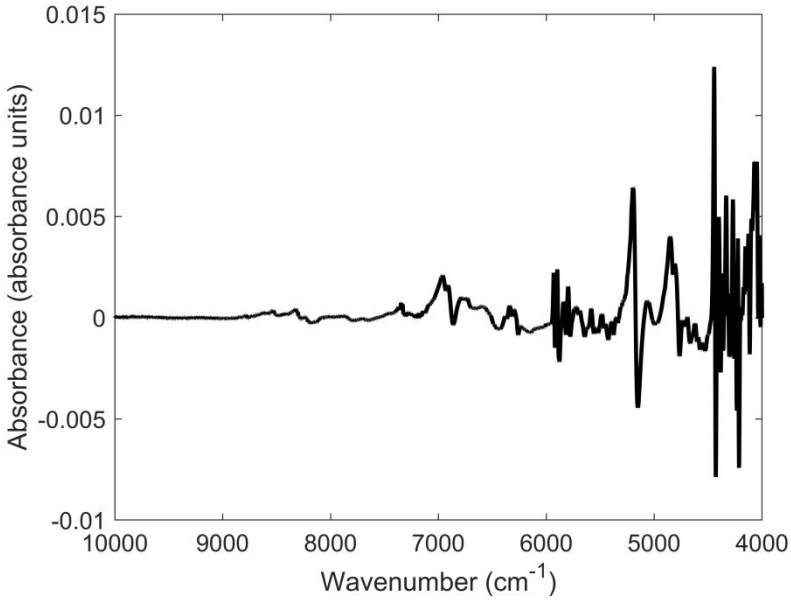

Figure B28. MSC-D1 NIR spectrum of lactose monohydrate measured using the Perkin Elmer Spectrum Two FT-NIR instrument equipped with NIRM.

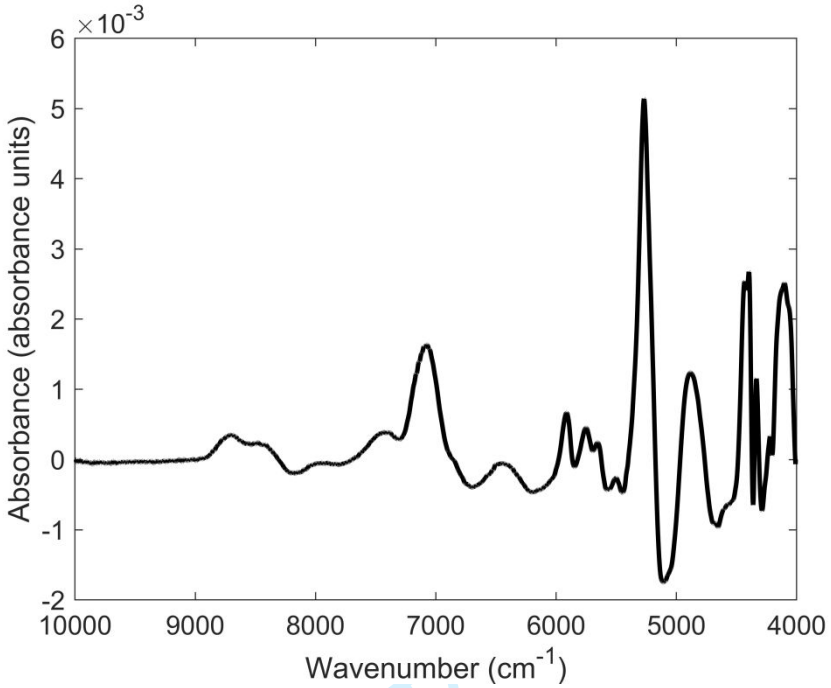

Figure B29. MSC-D1 NIR spectrum of maize starch measured using the Perkin Elmer Spectrum Two FT-NIR instrument equipped with NIRM.

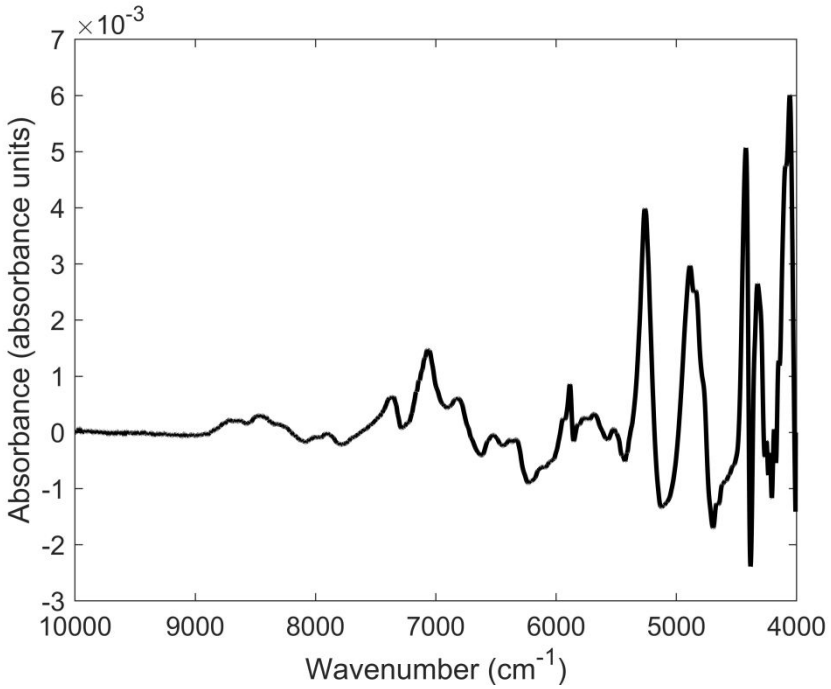

Figure B30. MSC-D1 NIR spectrum of microcrystalline cellulose measured using the Perkin Elmer Spectrum Two FT-NIR instrument equipped with NIRM.

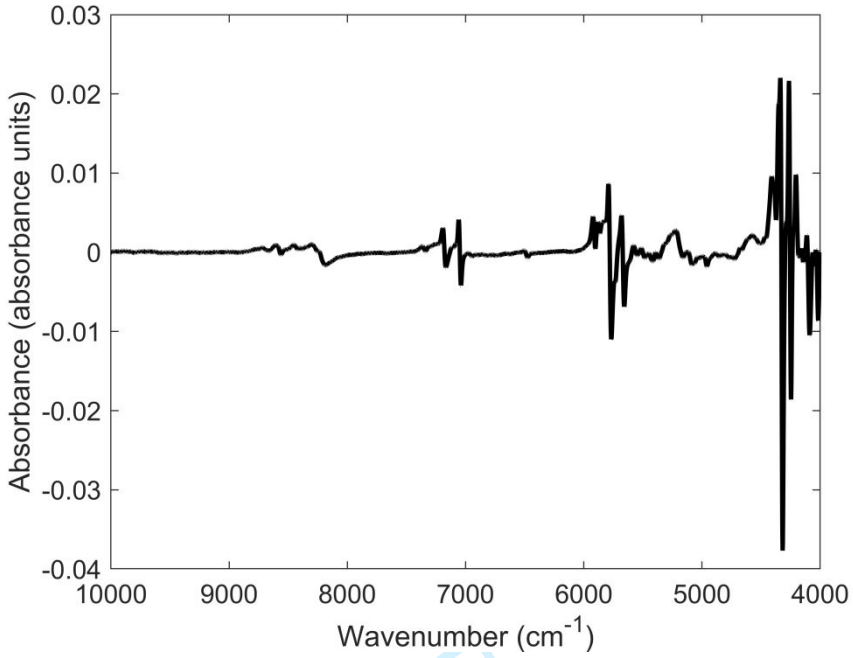

Figure B31. MSC-D1 NIR spectrum of magnesium stearate measured using the Perkin Elmer Spectrum Two FT-NIR instrument equipped with NIRM.

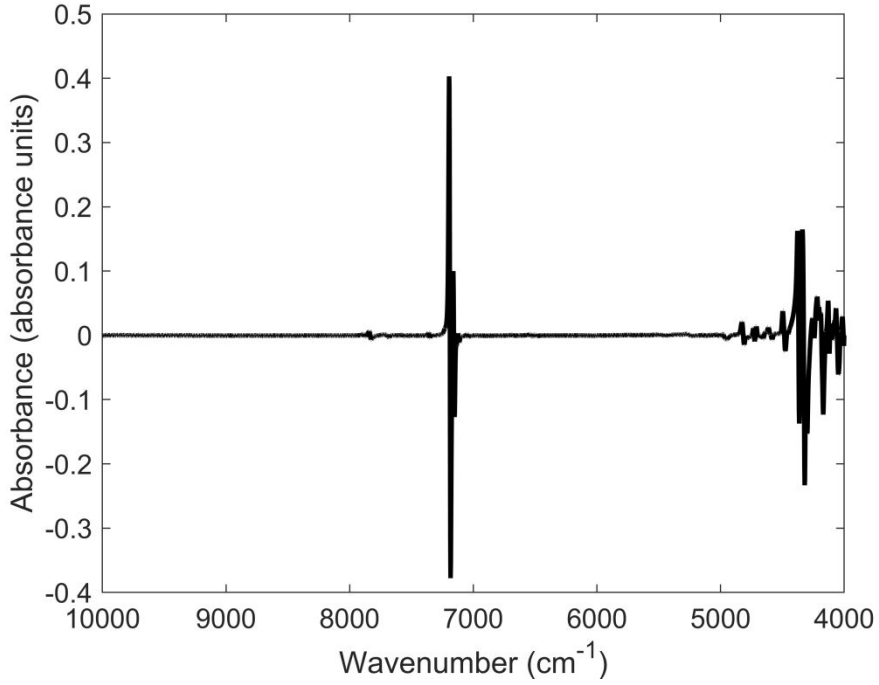

Figure B32. MSC-D1 NIR spectrum of talc measured using the Perkin Elmer Spectrum Two FT-NIR instrument equipped with NIRM.